HAL
open science

Predictive airframe maintenance strategies using model-based prognostics

Yiwei Wang, Christian Gogu, Nicolas Binaud, Christian Bes, Raphaël Haftka, Nam-Ho Kim

To cite this version:

Yiwei Wang, Christian Gogu, Nicolas Binaud, Christian Bes, Raphaël Haftka, et al.. Predictive airframe maintenance strategies using model-based prognostics. Proceedings of the Institution of Mechanical Engineers, Part O: Journal of Risk and Reliability, 2018, 232 (6), pp.690-709. 10.1177/1748006X18757084 . hal-01940475

HAL Id: hal-01940475

https://ut3-toulouseinp.hal.science/hal-01940475v1

Submitted on 27 Aug 2020

HAL is a multi-disciplinary open access archive for the deposit and dissemination of scientific research documents, whether they are published or not. The documents may come from teaching and research institutions in France or abroad, or from public or private research centers.

L'archive ouverte pluridisciplinaire **HAL**, est destinée au dépôt et à la diffusion de documents scientifiques de niveau recherche, publiés ou non, émanant des établissements d'enseignement et de recherche français ou étrangers, des laboratoires publics ou privés.

Predictive airframe maintenance strategies using model-based prognostics

Yiwei Wang[a], Christian Gogu[a,*], Nicolas Binaud[a], Christian Bes[a], Raphael T. Haftka[b] and Nam H. Kim[b]

[*]Corresponding author e-mail: christian.gogu@gmail.com

[a]Université de Toulouse, INSA/UPS/ISAE/Mines Albi, ICA UMR CNRS 5312, Toulouse, 31400, France

[b]Department of Mechanical & Aerospace Engineering, University of Florida, Gainesville, 32611, USA

Abstract

Currently, aircraft maintenance is highly regulated based on fixed schedules. At the scheduled maintenance time, the panel repair policy decides on repair based on damage size. This is very conservative due to the fact that the repair threshold is determined to ensure a desirable reliability for the entire fleet and due to the fact that the same damage size will evolve differently on different panels due to material variability. With the progress of sensor technology, data acquisition and storage techniques as well as advanced data processing algorithms, structural health monitoring (SHM) systems are increasingly being considered in the aviation industry. Aiming at reducing the conservativeness to reduce the maintenance cost, a model-based prognostics method developed in our previous work is employed here to predict future damage growth for each panel individually and to allow repair criteria according to future rather than present damage size. Based on the developed prognostics method, two predictive maintenance strategies are developed and applied to fatigue damage propagation in fuselage panels where the parameters of the damage growth model are unknown and the information on damage evolution is given by noisy SHM measurements. A numerical case study simulating the maintenance process of an entire fleet of aircraft is implemented, in which the uncertainty of damage model parameters among the panel population as well as the uncertainty of pressure differential during the damage propagation process is considered. The advantage of the predictive maintenance strategies is assessed through a cost model by comparing with other maintenance strategies. The results indicate that the proposed predictive maintenance strategies reduce significantly the unnecessary repair, thus lead to cost saving.

Keywords

Structural airframe maintenance, model-based prognostics, predictive maintenance, Extended Kalman filter, first-order perturbation method

Introduction

Aircraft maintenance represents a major economic cost for the aviation industry. In 2015, the Maintenance, Repair, Overhaul (MRO) market was three-quarters of the whole aircraft production market. Developing efficient maintenance can be an important way for airlines to allow a new profit growth. Aircraft maintenance can be classified into airframe maintenance and engine maintenance. Airframe maintenance that deals with non-structural items is called non-structural airframe maintenance [1] while the one that concerns the fatigue damage in the structural sections such as fuselage panels is called structural airframe maintenance. In this paper, the maintenance is limited to structural airframe maintenance, or more specifically, the maintenance for fatigue cracks in fuselage panels.

Traditionally, aircraft maintenance is highly regulated based on fixed maintenance schedule (thus called scheduled maintenance) in order to ensure safety and correct functionality during flight. For example, under Federal Aviation Administration (FAA), operators are required to prepare a mandatory Continuous Airworthiness Maintenance Program (CAMP). CAMP includes both routine and detailed inspections, which are generally referred to as "checks" by Airlines. There are four levels of "checks", termed as A, B, C and D, from lighter to heavier. A and B checks are lighter checks from dozens of man-hours to hundreds of man-hours, while C and D checks are heavy checks, during which the aircraft is partially disassembled to undergo a series of maintenance activities including both engine and airframe maintenance. The inspections are often implemented by techniques such as Non-Destructive Inspection (NDI), General Visual Inspection (GVI), Detail Visual Inspection (DVI), etc., which can lead to significant downtime up to one month.

With progress in sensor technology, structural health monitoring (SHM) systems, which employ a sensor network sealing inside aircraft structures to monitor the damage state, are gradually being introduced in the aviation industry.[2-5] Once it is possible to monitor the structure damage state automatically and continuously by an SHM system, more advanced condition-based maintenance (CBM) can be implemented instead of the scheduled maintenance.[6] CBM is defined by the maintenance being subordinated to an event and being triggered when some conditions are satisfied, e.g., the system state exceeds some thresholds. For structural airframe maintenance, CBM plans maintenance based on the actual condition of the aircraft, rather than fixed inspection routines that might not be necessary, and thereby reduces aircraft's downtimes and save the maintenance cost.

Much attention has been paid to CBM strategies in the literature [7-9] and more recently to predictive maintenance.[10-15] CBM and predictive maintenance share some characteristics in common that both of them rely on the damage-associated data collected by the SHM system. The difference lies in that in CBM, the maintenance decision-making relies only on current damage level while the predictive maintenance makes use of, in addition to current damage information, the prognostics index to support the decision-making. The remaining useful life (RUL) is the most common prognostics

index.[16] The RUL-based predictive maintenance decides the next maintenance dynamically based on estimated remaining useful life.[14, 17, 18] For aircraft maintenance, however, the standards are set by the International Civil Aviation Organization (ICAO) and implemented by national and regional bodies around the world. Arbitrarily deciding the structural airframe maintenance time only based on the estimated RUL of structures without taking into account the scheduled maintenance (during which the engine and non-structural airframe maintenance are performed) can be quite disruptive to current maintenance practice. In addition, the arbitrary triggered maintenance is unexpected and less optimal from the economic point of view due to less notification in advance, e.g., the absence of maintenance crew, the lack of a spare part, etc. Therefore, for structural airframe maintenance that this paper concerns, it would be more desirable to predict the probability that an airframe structure operates normally up to some future time.[19] In other words, use the "predicted reliability" as the prognostics index. The predictive maintenance policy that incorporates the "predicted reliability" information for supporting decision-making can be found in.[10, 13, 15]

For the application of structural airframe maintenance for an aircraft fleet in airlines, Pattabhiraman [1] proposed two CBM strategies, which aim at reducing the number of traditional scheduled maintenance. One strategy is purely CBM, i.e., triggering maintenance anytime when needed only based on the current panel health state without considering the recommended maintenance schedule, while the other strategy does take into account the schedule. In their approach, an SHM system is used to monitor the damage state of the aircraft as frequently as needed. Using the measurements of crack size, the maintenance decisions are developed based on some fixed thresholds. These thresholds are determined for the entire fleet of aircraft to ensure a desirable level of reliability. There are two shortcomings in the work of Pattabhiraman et al. First, they assume the SHM data are perfect, which may be less practical since due to the sensor limitations and harsh working conditions, the data always contain noise and disturbances. Second, Pattabhiraman used two different thresholds, corrective threshold and preventive threshold to distinguish a corrective repair and a preventive repair (the preventive threshold is much smaller than the corrective one). Corrective repair is carried out when the damage level of the panels exceed the corrective threshold. Preventive repair is carried out at the time of corrective repair to preventatively repair the panels whose damage level exceed the preventive threshold but may be far less than the corrective threshold. The objective of predictive repair is for economic reasons, e.g., to reduce maintenance stops to save the setup cost. Although Pattahiraman considered two types of repair, the corrective threshold and the preventive threshold are fixed for all the panels in the fleet. This could be less optimal since the damage growth rate may vary from panel to panel. Therefore, a conservative threshold should be adapted to ensuring the safety of the whole fleet.

This paper thus aims to go further in terms of optimizing the maintenance process, by moving from condition-based maintenance as proposed in Pattabhiraman's work to predictive maintenance, which has the potential for further cost savings. We therefore adopt the second type of prognostics index, i.e., the "*predicted reliability*", for supporting maintenance decision-making to reduce the conservativeness caused by the use of fixed thresholds for the entire fleet. To this end, we use a model-based prognostics method,

called EKF-FOP method that couples the Extended Kalman filter (EKF) and First-Order Perturbation (FOP), developed in our previous work.[20] EKF-FOP allows to make the repair decision taking into account the future reliability of each individual panel rather than a fixed threshold for all the panels. The EKF-FOP method has two functions: filtering the measurement noise to give a better estimate of damage level (achieved by EKF) and predicting the damage distribution in future time (achieved by FOP). Once the damage distribution of a panel is predicted, the reliability of the panel in future time is calculated. This "predicted reliability information" is used to form the repair policy, which is the core of the predictive maintenance presented in this paper. Similar to Pattabhiraman, we proposed two strategies: the purely predictive maintenance called PdM without considering the aircraft scheduled maintenance and the one called PdM-skip, who takes into account the maintenance schedule. The performance of PdM and PdM-skip is assessed through a cost model by comparing with Pattabhiraman's two CBM strategies as well as with the traditional scheduled maintenance.

The remainder of this paper is organized as follows. Section 'Model-based prognostics for individual fuselage panel' briefly recalls the model-based prognostics method proposed in Ref. [20] for the application of fatigue crack prognosis. Section 'Predictive maintenance strategies using model-based prognostics' details the developed predictive maintenance strategies when the model-based prognostics method is integrated. Section 'Numerical examples' implements the numerical experiments on a fleet of short-range commercial aircraft. Benefits of the integration of model-based prognostics are shown in terms of scheduled and unscheduled repair as well as maintenance cost reduction. Finally, in the last section we draw conclusions and suggest potential future research work.

Model-based prognostics for individual fuselage panel

Prognostic methods can generally be grouped into data-driven and model-based methods. For the application of fatigue crack prognosis, the model-based method is adopted here since the fatigue damage models for metals have been well researched.[21, 22] Model-based prognostics methods involve three issues. (1) A physical model with unknown model parameters describing the degradation process is assumed available. (2) The damage state and the model parameters need to be estimated from the measurement data collected sequentially up to the current time. (3) Predicting the distribution of future damage state from the current time, based on the estimated damage state and model parameters in the second issue.

For the first issue, the well-known Paris model is used for fatigue crack propagation, as given in Eq.(1), in which a is the half-crack size in meters, k is the number of load cycles, $\mathrm{d}a/\mathrm{d}k$ is the crack growth rate in meter/cycle. m and C are the Paris model parameters that are also referred to as material parameters. Throughout this paper, we use the terms "Paris model parameters", "model parameters" and "material parameters" interchangeably to refer to m and C. ΔK is the range of stress intensity factor, which is given in Eq.(2) as a function of the pressure differential p, fuselage radius r and panel thickness t. The coefficient A in the expression of ΔK is a correction factor intended

to compensate for modeling the fuselage as a hollow cylinder without stringers and stiffeners.[1] The two model parameters m and C are assumed unknown that need to be estimated from the measurement data.

$$\frac{da}{dk} = C(\Delta K)^m \tag{1}$$

$$\Delta K = A\frac{pr}{t}\sqrt{\pi a} \tag{2}$$

The crack growth can be modeled in myriad ways depending on whether the critical site is subjected to multiple-site damage (MSD), widespread fatigue damage (WFD), two-bay crack or other types of fatigue damage. Based on a study conducted by Molent et al.,[23] in which the author reviewed fatigue crack growth data from a significant number of full-scale fatigue test (FSFT) on several different military aircraft types. In the FSFT, the airframe was subjected to loads of varying amplitude and complexity for a specified period of testing. As the result of the review, Molent et al. concluded that a simple crack growth model adequately represents a typical crack growth. Here the well-known Paris model is employed since it is widely used for modeling fatigue crack growth.[24, 25]

For the second issue, several techniques can be considered, e.g., Extended Kalman filter (EKF), Particle filter (PF), Nonlinear Least Squares (NLS), etc. EKF and PF are based on recursive Bayesian inference, which estimate the state and parameters recursively by taking one data at a time.[26] Therefore, they are able to deal with the real-time estimation of state and parameters as the data arrive sequentially. In contrast, NLS processes all data simultaneously in a batch way, indicating that the computational complexity increases as time evolves and as more data are available. In this paper, the crack propagation process is modeled as a Hidden Markov model (HMM, or general state-space model [27]) since we assume that the evolution of crack size is hidden but can be observed through measurement data that contain noise. HMM is widely used to model the degradation process.[28, 29] In this sense, filter methods are more appropriate. Here EKF is chosen due to its time efficiency and robustness. EKF gives the estimates of crack size and model parameters as well as their uncertainty (represented by the covariance matrix). Note that identifying the uncertainty structure (covariance matrix) is necessary in order to be able to estimate the future reliability index.

For the third issue, once the state and parameters are estimated, the future behavior of degradation can be easily predicted. A straightforward way is Monte Carlo (MC) simulation, i.e., generate a certain number of samples based on the estimated joint distribution of state-parameter given by EKF in the second issue and propagate these samples through the Paris model for a given amount of future time. The idea of using MC simulation is illustrated in Figure 1. Alternatively, we proposed a linearization method called first-order perturbation (FOP) method to calculate the evolution of crack size distribution analytically. One advantage of the FOP method over the Monte Carlo simulation is its ability to save computational cost. This advantage might not be obvious when dealing with one individual crack growth process in one fuselage panel but is

significantly meaningful when applying the discussed model-based prognostics on a fleet of aircraft comprising hundreds or thousands of aircraft.

The process of modelling the crack propagation as an HMM and the details of the developed EKF-FOP method were presented in the Sections 2 and 3 in Ref. [20]. For sake of completeness, the method is recalled in Appendix 1. Only the necessary notations for the following narrative are presented here. The crack size and two Paris model parameters estimated by EKF at cycle k are denoted as $\hat{a}_k$, $\hat{m}_k$ and $\hat{C}_k$, respectively. The predicted mean and standard deviation of the crack size given by FOP method after h cycles further from the current cycle k is denoted as μ_{k+h} and σ_{k+h}. The schematic diagram of EKF-FOP method is illustrated in Figure 2.

In order to verify the accuracy of the proposed FOP method for future degradation prediction, we compare the predicted crack size distribution given by FOP method and the one given by MC simulation in a certain amount of time beyond the last measurement. The comparison is detailed in Appendix 2. We find that the predicted mean and standard deviation with the FOP method are within a few percent of those predicted by the MC method, however the FOP method involves a computational cost, which is about 4800 times lower than MC. Moreover, we evaluate the performance of the EKF-FOP method by comparing with true known remaining useful life (RUL) using five established prognostics metrics[30]: prognostics horizon (PH), $\alpha - \lambda$ accuracy, relative accuracy (RA), cumulative relative accuracy (CRA), and convergence. The results are reported in Appendix 3. The results show that the proposed prognostics method performs well according to all five prognostic metrics.

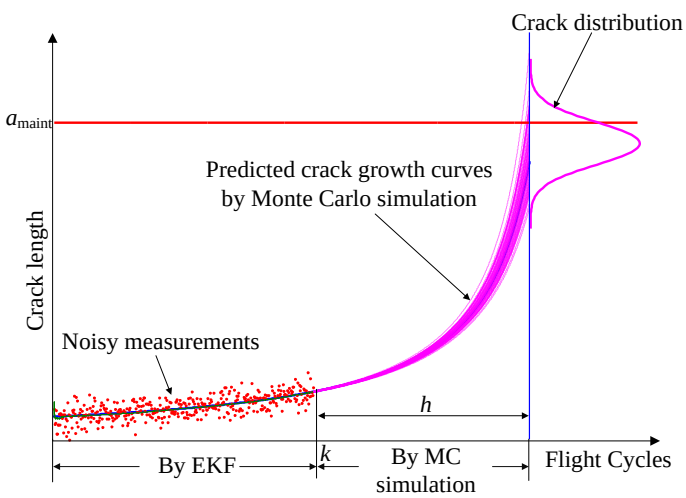

Figure 1. Using Monte Carlo method to predict the future behavior of degradation

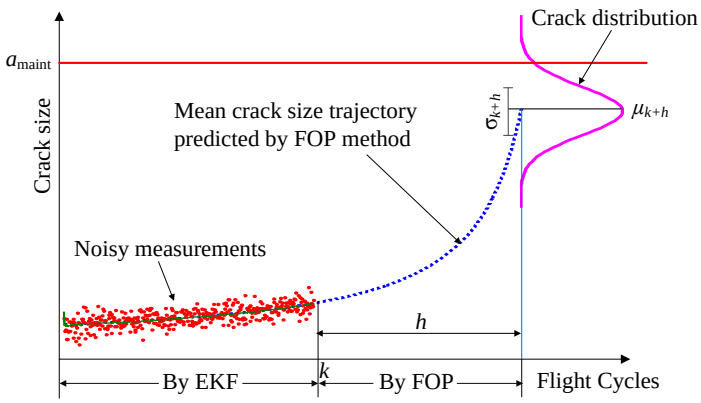

Figure 2. Schematic diagram of EKF-FOP method

Predictive maintenance strategies using model-based prognostics

In this section, two variants of predictive maintenance strategies are developed using the model-based prognostics method introduced in the previous section. Remainder that our objective is to plan the structural airframe maintenance while the engine and non-structural airframe maintenance are always performed at the time of scheduled maintenance.

Maintenance assumptions

The employment of SHM system leading the possibility of planning the maintenance based on the actual health state of the aircraft rather than a fixed schedule. However, as mentioned before, arbitrarily triggering maintenance might be a bit disruptive to the traditional scheduled maintenance, during which the engine and non-structural airframe maintenance are carried out. On the other hand, it makes sense to skip some scheduled maintenance at the near stage of the aircraft lifecycle since the frequency of scheduled maintenance for commercial aircraft is designed very conservative. It is highly likely that no panels need to be repaired at the earlier stage of the aircraft lifecycle. In summary, it would be beneficial that scheduled maintenance work in tandem with the scheduled maintenance.

For the scheduled maintenance, the aircraft undergoes the routine maintenance according to the schedule $T_b = T_1 + (b\text{-}1)\Delta T$, where b is an integer indicating the number of maintenance stops, T_1 the flight cycle of the first scheduled maintenance stop, and ΔT the interval between two consecutive scheduled maintenance. The schedule $\{T_b\}$ is defined by aircraft manufacturers in concertation with certification authorities. Therefore, it is assumed to be fixed.

SHM system is assumed to monitor the damage state of each panel in the fuselage. The frequency of damage status evaluation, henceforth called damage assessment, is assumed every 100 flights, which is coincided with A-check. It would make sense to carry out the SHM-based maintenance as a frequency of 100 cycles if the

sensors themselves are embedded in the aircraft and the monitoring system is ground-based to reduce flying weight and monitoring system cost.[1]

Although our application objective is a fuselage that contains hundreds of panels, panels are treated independently and their structural dependency is not considered. That makes sense because unlike the system having a *k*-out-of-*n*: F structures (i.e., the system fails if at least *k* of the n components fail) or the (*n*-*k*+1)-out-of-*n*: G structures (the system works if at least (*n*-*k*+1) of the *n* components work), the malfunction of one panel does not affect that of other panels. One can refer to Ref. [10, 14] for the maintenance policy considering structural dependency.

The critical half crack size that will cause a panel failure can be calculated by Eq.(3). Based on linear elastic fracture mechanics, equaling the stress intensity factor in mode I (cf. Eq.(2)) to the fracture toughness K_{IC} leads to the critical crack size a_{cr} as shown in Eq.(3), where p_{cr} is a conservative estimate of the pressure differential. Since the damage assessment is done every 100 cycles and no intervention is performed between 100 cycles, an additional safety threshold, denoted as a_{maint}, is introduced to maintain a desirable reliability between 100 cycles. a_{maint} is calculated to maintain a 1e-7 probability of failure of the aircraft between two damage assessments, i.e., when a crack size exceeding a_{maint} is present on the aircraft, its probability to exceed the critical crack size a_{cr} in future 100 cycles is less than 1e-7. A 1e-7 probability of failure is a typical reliability used in aircraft damage tolerance design and is referred in literatures.[1, 31] By repairing panels having cracks larger than a_{maint}, one ensures the safety of the aircraft until next damage assessment.

$$a_{\mathrm{cr}} = \left(\frac{K_{\mathrm{IC}}}{A \frac{p_{\mathrm{cr}} r}{t} \sqrt{\pi}} \right)^2 \tag{3}$$

Repair policy for individual crack propagation process

The EKF-FOP method introduced in the previous section is used to develop the repair policy. According to EKF-FOP method, when measurement data are available up to the *k*-th cycle, the EKF is used to estimate the crack size and to identify the Paris model parameters at the *k*-th cycle. Based on the estimated crack size and material parameters, i.e. $\hat{a}_k$, $\hat{m}_k$ and $\hat{C}_k$, the FOP method is used to predict the evolution of the crack size in the future *h* cycles. As per EKF-FOP, the distribution of the crack size is a normal distribution. The mean and standard deviation of the crack size at *k*+*h*, μ_{k+h} and σ_{k+h}, are calculated by the FOP method. Based on the predicted crack size distribution, we calculate the 0.95 quantiles, denoted by a_{q}.

$$a_{\mathrm{q}}(h) = \Phi^{-1}(0.95 \mid \mu_{k+h}, \sigma_{k+h}) \tag{4}$$

in which Φ^{-1} is the inverse cumulative distribution function of the normal distribution with mean and standard deviation μ_{k+h} and σ_{k+h}, respectively. If $a_q > a_{maint}$, the panel is considered in danger and should be repaired. Otherwise, this panel is left unattended. This "repair decision" is denoted as d, which could be considered as a binary value.

$$d = \begin{cases} 0 & if\ a_q \le a_{maint} \\ 1 & if\ a_q > a_{maint} \end{cases} \tag{5}$$

The underlying meaning behind the repair policy is that if a crack size equaling $\hat{a}_k$ is present on the panel, the probability that this crack grows greater than the threshold a_{maint} at the next scheduled maintenance is less than 5%. Note that the level of the quantile (95% here) controls the conservativeness of the estimation and can be seen as a tuning parameter of the strategy. This conservativeness level is not however intended to guarantee the safety of the aircraft. The safety of the aircraft will be guaranteed by an additional branch of the maintenance strategy as will be described later. Through an empirical study, we found that the cost of the proposed maintenance strategies is relatively insensitive to the value of the quantile, so in the rest of the paper this value is fixed to 95%. Note also that the forward prediction interval h varies depending on different strategies and can be seen as another tuning parameters of the strategy. This tuning parameter was found more sensitive and its tuning will be addressed in the subsequent sections.

Predictive maintenance (PdM)

The objective of PdM is to decide the maintenance according to the actual condition of an aircraft rather than based on a fixed maintenance schedule. Figure 3 illustrates the flowchart of PdM. In this strategy, damage assessment is implemented every 100 cycles. At each damage assessment, the EKF is used to calculate the estimated crack size of all the panels in an aircraft. If the largest crack size exceeds a_{maint}, an unscheduled maintenance is asked immediately and this aircraft is sent to the maintenance hangar. The panel with the largest crack size triggering the unscheduled maintenance is called critical panel. At the stop of unscheduled maintenance, besides repairing the critical panel, other panels may be also repaired according to the repair policy presented in the previous subsection to prevent frequent unscheduled maintenance. More specifically, for the i-th panel, its crack size distribution in the next $h=I_{PdM}$ cycles is predicted and the 0.95 quantiles of the predicted crack size, denoted as $a_q^i(I_{PdM})$, is calculated. The panels whose $a_q^i(I_{PdM})$ is greater than a_{maint} are repaired. The value of forward prediction interval I_{PdM} can be optimized. Following an empirical study with different I_{PdM} values we set I_{PdM}=23000 cycles which was found to lead to the lowest maintenance costs.

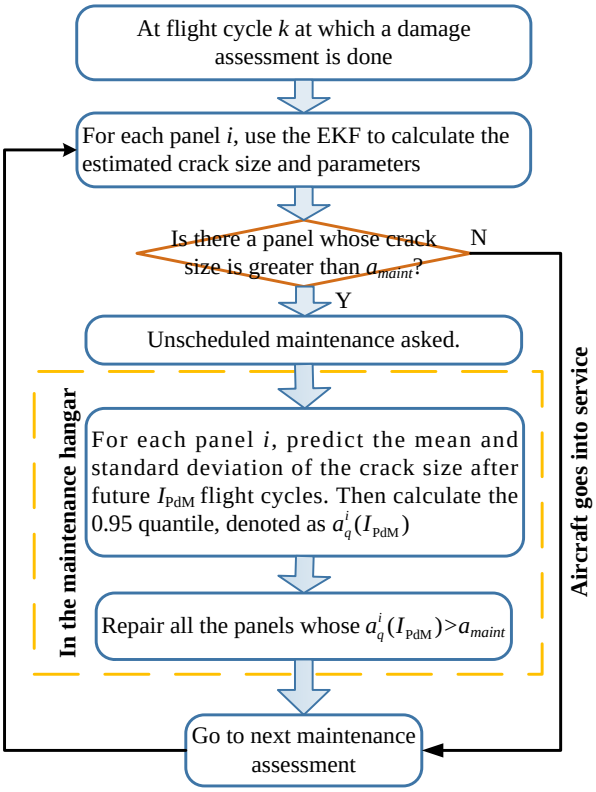

Figure 3. Flowchart of PdM strategy for an aircraft

Predictive maintenance-skip (PdM-skip)

Despite the advantage of PdM, it also has some drawbacks. The predictive maintenance applies only to structural airframe maintenance. The engine and non-structural airframe maintenance are always implemented at scheduled maintenance. Predictive maintenance that triggers unscheduled maintenance may disturb the original scheduled maintenance. In addition, having the structural airframe maintenance as much as possible at the same time with the engine and non-structural maintenance would tend to reduce cost. Therefore, it is beneficial that in civil aviation industry the traditional scheduled maintenance works in tandem with the unscheduled maintenance. PdM-skip is developed to meet this goal that leverages the strength from both scheduled maintenance and PdM.

The PdM-skip process is described in Figure 4. The damage assessment is carried out at scheduled maintenance time as well as every 100 cycles. At each scheduled maintenance stop, for an aircraft, there are two decisions levels. The first level is maintenance decision that decides to skip or to trigger the current scheduled maintenance for the aircraft. The second level decision is repair decision regarding which panels should be repaired once the current scheduled maintenance is triggered.

Specifically, the maintenance decision is implemented as follows. At each scheduled maintenance, before the aircraft goes to the maintenance hangar, for the i-th panel, its crack size distribution after next $h=\Delta T$ cycles is predicted (i.e., the distribution at next scheduled maintenance) and the 0.95 quantiles of the predicted crack size

distribution, denoted as $a_{\mathrm{q}}^{i}(\Delta T)$, is calculated. If there is no panel whose $a_{\mathrm{q}}^{i}(\Delta T)$ exceeds a_{maint}, the current scheduled maintenance is skipped. Otherwise, the current scheduled maintenance is triggered and the aircraft is sent to the maintenance hangar. The objective of setting the forward prediction interval $h=\Delta T$ is to avoid unscheduled maintenance between two consecutive scheduled maintenance stops.

For the aircraft having been sent to the hanger, the repair decision is implemented as follows for all the panels of the aircraft. For the *i*-th panel, its crack size distribution until the end of life (EOL) of the aircraft is predicted, that is to say, the forward prediction interval h equals to the aircraft lifetime, denoted as k_{EOL}, minus the current number of cycles k, i.e., $h=k_{\mathrm{EOL}}-k$. The 0.95 quantile of the predicted crack size distribution, denoted as $a_{\mathrm{q}}^{i}(k_{\mathrm{EOL}}-k)$, is calculated. All the panels whose $a_{\mathrm{q}}^{i}(k_{\mathrm{EOL}}-k)$ exceed a_{maint} are repaired.

If a crack that is missed at the time of scheduled maintenance exceeds a_{maint} between two consecutive scheduled maintenances, PdM-skip will recommend maintenance to be performed immediately. This calls for unscheduled maintenance, which is costlier but guarantees safety. At unscheduled maintenance stop, we predict the crack size distribution in the future I_c cycles for all panels and then decide the ones that need to be repaired according to the repair policy. I_c is set to be the number of cycles from current to the scheduled maintenance after the next one. This is to be able to skip the next scheduled maintenance and not have an unscheduled maintenance soon after. For example, if the scheduled maintenance is every 4,000 cycle and an unscheduled maintenance occurs at the 43,000th cycle, I_c will be set to 5,000 in order to have the next maintenance at 48,000 cycles by skipping the one at 44,000 cycles.

Cost model

The aircraft maintenance cost is composed of engine maintenance cost and airframe maintenance cost. The airframe maintenance cost is further divided into structural airframe and non-structural airframe maintenance. In this paper, we focus on structural airframe maintenance cost. Note that the engine and non-structural maintenance are always performed at the time of scheduled maintenance interval. The cost of the structural airframe maintenance performed by traditional NDI or DVI technologies at the time of scheduled maintenance stop consists of two parts, the setup cost c_0 and the repair cost. The repair cost equals the cost of repairing one panel, denoted by c_s, multiplied by the number of repaired panels. c_0 is assumed 1.44 and c_s is \$0.25 million as per Ref.[32].

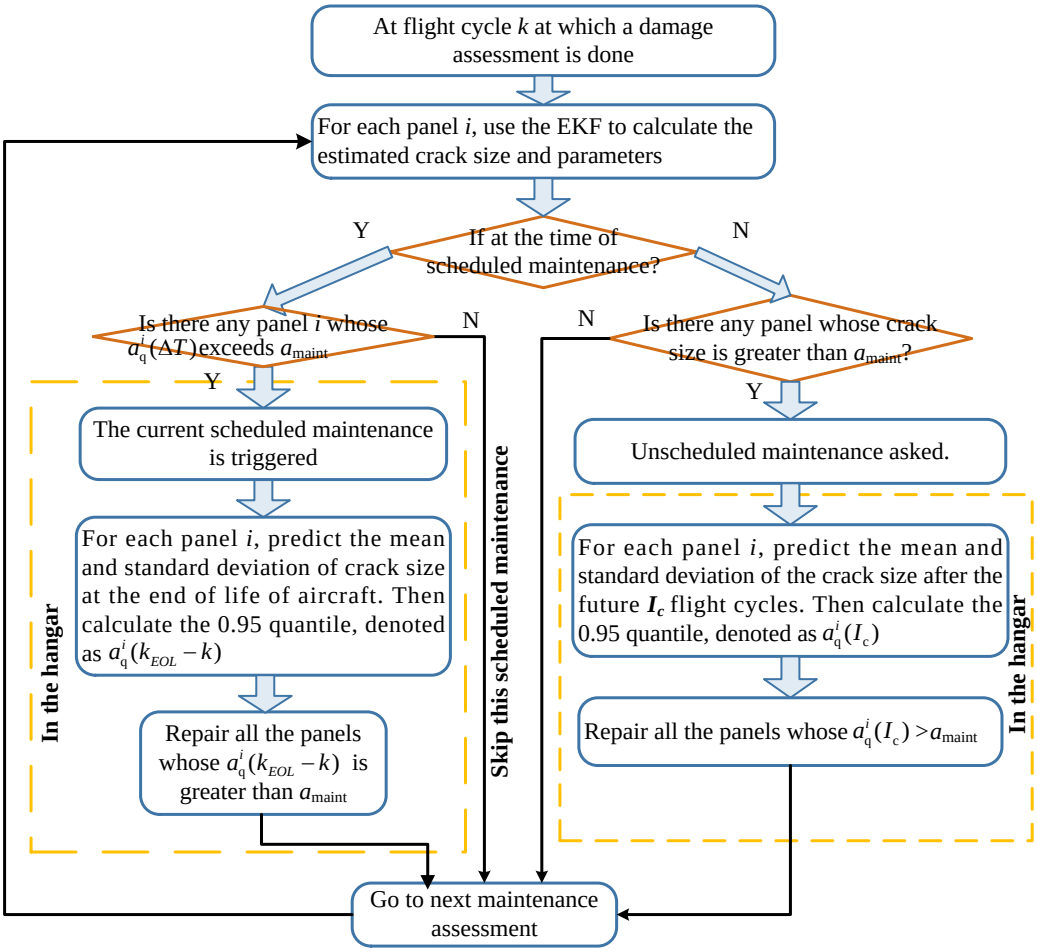

Figure 4. Flowchart of PdM-skip strategy

In the PdM and PdM-skip, the damage inspection is performed by the on-board SHM system, hence at the scheduled maintenance, the setup cost will be only a fraction compared to the cost of the traditional scheduled maintenance. This fraction is denoted as K_{SHM} and is set to be 0.7.[1] The setup cost at an unscheduled structural airframe maintenance trip is higher due to less advance notice, as well as the fact that the structural airframe maintenance and the other maintenance (engine, non-structural) are not done at the same time. A factor, K_{un} is set to denote the higher setup cost incurred for unscheduled maintenance and K_{un}=2 is taken.[1] The cost of structural airframe maintenance is thus given as

$$C_{\mathrm{main}} = N_{\mathrm{s}} K_{\mathrm{SHM}} c_0 + N_{\mathrm{us}} K_{\mathrm{un}} c_0 + c_{\mathrm{s}} N_{\mathrm{rp}} \tag{6}$$

where N_{s} is the number of triggered scheduled maintenance, N_{us} the number of unscheduled structural maintenance trips, N_{rp} the number of repaired panels in the whole lifetime of an aircraft.

Numerical examples

Our application objective is a typical short-range commercial aircraft with a typical lifetime of 60,000 flight cycles. We consider a fleet of 100 such airplanes with 500 fuselage panels per aircraft. Each panel is assumed to have one initial crack, with initial crack size following a lognormal distribution. Traditionally, the maintenance schedule of this type of aircraft is designed such that the first maintenance is performed after 20,000 flight cycles and the subsequence maintenance is every 4,000 cycles until its end of life, thus adding up to 10 scheduled maintenance stops throughout its lifetime, as shown in Figure 5.

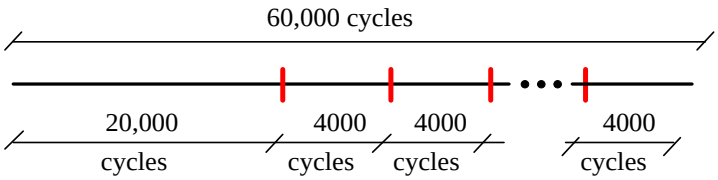

Figure 5 Scheduled maintenance, cycles represent the number of flights

We evaluate the performance of PdM/PdM-skip by comparing with two other strategies. The first strategy is the traditional scheduled maintenance, whose schedule is shown in Figure 5. At each scheduled stop, the aircraft is taken into a hangar and the inspection of all panels is done using techniques like NDI or DVI. Cracks detected with a size greater than a threshold are repaired. The threshold is determined to guarantee a desirable level of probability of failure between two scheduled maintenances and is fixed for all panels in the fleet. Therefore, this strategy is threshold-based.

The second strategy has two variants due to Pattabhiraman.[1] CBM and CBM-skip, in which the damage assessment is done every 100 flights by using SHM. Details about CBM and CBM-skip are given in Appendix 4. In CBM, at each damage assessment, if the largest crack size in an aircraft exceeds a_{maint}, unscheduled maintenance is trigged immediately and all the panels with a crack size larger than a repair threshold $a_{\text{rep-CBM}}$ are repaired.

In contrast, CBM-skip takes into account the scheduled maintenance but aims at skipping some unnecessary early scheduled maintenance. Specifically, at each scheduled maintenance stop, if there is no crack size exceeding a threshold $a_{\text{th-skip}}$, then the current scheduled maintenance is skipped. Otherwise, the current scheduled maintenance is triggered and the panels with crack size greater than a repair threshold $a_{\text{rep-skip}}$ are repaired. If there is a crack grows beyond a_{maint} between two consecutive scheduled maintenance then an unscheduled maintenance is trigged at once and all panels with crack size greater than $a_{\text{rep-skip}}$ are repaired.

CBM and CBM-skip are also threshold-based since the thresholds are fixed for the entire fleet. Since our work is an extension of Pattabhiraman's, we seek to compare the threshold-based maintenance and our prognostics-based maintenance. Note that in CBM and CBM-skip, the reliability is controlled by the safety threshold a_{maint} while $a_{\text{rep-CBM}}$, $a_{\text{rep-skip}}$ and $a_{\text{th-skip}}$ are tuning parameters affecting the cost that can be optimized. The

same value of a_{maint} is used in CBM, CBM-skip, PdM and PdM-skip, that is to say, all strategies are compared under the same safety level.

Besides the strategies themselves, another significant difference between Pattabhiraman's work and our work is the treatment to the pressure p. Pattabhiraman treated it as a constant while we have taken into account its uncertainty during the crack propagation and modeled it as a normal random variable. In order to maintain consistency and to make our work comparable, we introduce the uncertainty of p into Pattabhiraman's strategies. Accordingly, the thresholds used in CBM/CBM-skip are modified to adapt to the introduction of uncertainty on p.

Input data

The values of the geometry parameters defining the fuselage (e.g. fuselage radius, panel thickness) used here are related to short-range commercial aircraft. These values are time-invariant. Recall that we define a correction factor A for stress intensity factor, which accounts for the fact that the fuselage is modeled as a hollow cylinder (without stringers and stiffeners). The numerical values for the geometry parameters have been chosen from [1] and are reported in Table 1.

Table 1. Aircraft geometry parameters

Description	Notation	Value
Fuselage radius	r	1.95 m
Panel thickness	t	2e-3 m
Correction factor	A	1.25

The values of thresholds are determined as follows. The critical crack size a_{cr} is calculated by Eq.(3) and a_{cr}=59.6mm. The safety threshold a_{maint} is calculated to maintain a 1e-7 probability of panel failure between two damage assessments (every 100 cycles) and a_{maint}=47.4mm. To make CBM and CBM-skip as cost-efficient as possible, it is necessary to find the optimal value of $a_{rep\text{-}CBM}$, and the optimal combination of $a_{rep\text{-}skip}$ and $a_{th\text{-}skip}$. For this purpose we carried out an empirical trade-off study by considering a grid within the range [2,15] mm for $a_{rep\text{-}CBM}$, [2,12] mm for $a_{rep\text{-}skip}$ and [2,15] mm for $a_{th\text{-}skip}$, all with an increment of 0.1mm. Based on the evaluations of these grid points we found that the values $a_{rep\text{-}CBM}$=4.8mm, $a_{rep\text{-}skip}$=4.0mm and $a_{th\text{-}skip}$=7.0mm lead to the lowest maintenance cost according to the cost model in Eq.(6).

For simulating maintenance process of a fleet, we consider two types of uncertainties that are different in nature, i.e., aleatory uncertainty and epistemic uncertainty.[33] Aleatory uncertainty represents the intrinsic variability among populations that cannot be reduced by further data. In our context, it can be interpreted as follows. Even if the panels are made of the same materials, the material parameters of different panels may not be exactly the same. In addition, due to the intrinsic variability in crack

initiation, each panel has different initial crack size. In this study, the aleatory uncertainty is modeled by assuming that the initial crack size a_0, the material parameters follow some predefined distributions. Specifically, the initial crack size a_0 is assumed lognormally distributed while m and $\log C$ are assumed to follow a multivariate normal distribution with a negative correlation coefficient, based on the research indicating that m and $\log C$ are negatively linearly correlated.[22, 34, 35] The predefined distributions are reported in Table 2. Before starting the simulation, 100×500 samples of initial crack size and the model parameters are randomly drawn from their respective distributions, and assigned to each panel. Specifically, the initial crack size is generated from the lognormal distribution while the two model parameters are generated from the multivariate normal distribution, and denoted as $a_0^{(i)}$, $m^{(i)}$ and $\log C^{(i)}$ (i=1,2,…50000), respectively. $m^{(i)}$ and $\log C^{(i)}$ are regarded as the "true but unknown" material parameters of an individual panel (here "unknown" means the material parameters contains epistemic uncertainty, which will be discussed after). The 50,000 generated samples of the materials parameters are illustrated in Figure 6.

Table 2. Uncertainties on a_0, [m, C]

Description	Notation	Type	Value
Initial crack size (meter)	a_0	Log normal	LnN(0.3e-3,0.08e-3)
Paris model parameters	[m, C]	Multivariate normal	N (μ_m, σ_m , μ_C , σ_C , ρ)
Mean of m	μ_m	-	3.6
Mean of C	μ_C	-	Log_{10}(2e-10)
CC[a] of m and C	ρ	-	-0.8
SD[b] of m	σ_m	-	3% COV[c]
SD of C	σ_C	-	3% COV

[a]CC means the correlation coefficient
[b]SD means standard deviation
[c]COV means coefficient of variation

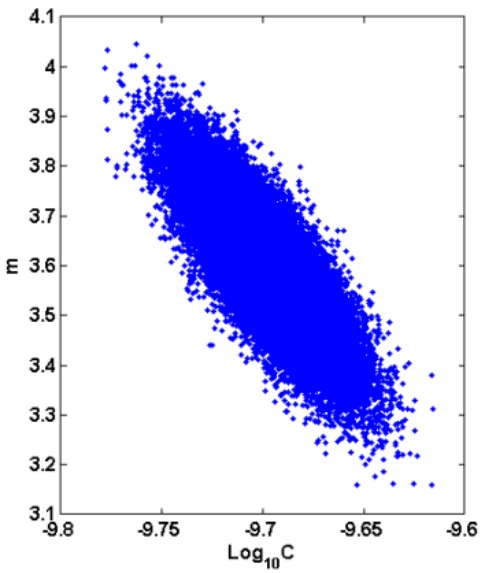

Figure 6. Illustration of the population of {*m C*}

The aleatory uncertainty relates to the variability in the population of the panels. Now we discuss the crack growth process in each individual panel. For an individual panel, its material parameters, $m^{(i)}$ and $\log C^{(i)}$, are not random in nature but deterministic. However, due to lack of knowledge, they are unknown or poorly known. This kind of uncertainty is referred to as epistemic uncertainty and can be reduced by collecting more relevant data. In our case, the material parameters are estimated from noisy measurements by the EKF algorithm, and furthermore, the estimation uncertainty reduces as time evolves due to more data being available.

The measurement data used in this paper are simulated as follows. (a) using $a_0^{(i)}$, $m^{(i)}$ and $\log C^{(i)}$ (i=1,2,…50000) to compute the true crack size based on Paris model, (b) adding the following measurement noise to the true crack size: Gaussian noise with mean zero and standard deviation sigma=0.03e-3(10% coefficient of variation with respect to the mean of initial true crack size in Table 2, i.e., 0.3e-3). The measurements are collected every 100 cycles, being consistent with the interval of damage assessment. At each time of damage assessment, the EKF is applied to estimate the crack size and the Paris model parameters. We choose Gaussian noise based on its wide use to simulate a realistic noisy signal. It is a good assumption for the process or system that is subject to the central limit theorem.[36] In the absence of information indicating otherwise, Gaussian noise is thus used to model measurement noise under the assumption of numerous sources of uncertainty and the central limit theorem.

It is difficult to get actual data on aircraft fuselage panel since the widespread deploy of SHM systems in commercial aircraft is still at the research stage. Tests have been done during the last decades by airlines as well as research centers. The major aircraft operators, regulators and technology suppliers have been striving for years to standardize SHM integration and certification requirements to mature system for widespread use. Therefore, at this stage, it is difficult to get real data to be used directly in our approach. Nevertheless, our work is built on realistic assumption based on existing

studies on fatigue crack propagation and can be used readily when measurements are available.

To summarize, we consider a fleet comprising 100 aircraft with each aircraft having 500 fuselage panels. The lifetime of each aircraft is assumed 60,000 cycles. Each panel is assumed to have one crack. EKF-FOP method is employed to each individual crack growth process in each panel. The developed two predictive maintenance strategies, PdM and PdM-skip, as well as the scheduled maintenance, CBM and CBM-skip are applied on the fleet until the end of the life of the aircraft. The average number of repaired panels, the average number of maintenance stops and the average structural airframe maintenance cost of the fleet under each strategy are obtained and compared.

Results and discussion

We simulate six processes, i.e., no maintenance intervention, scheduled maintenance, CBM, CBM-skip, PdM, and PdM-skip. It should be noted that in the "no maintenance intervention" process, the failure of a panel is defined such that the crack size in that panel exceeds a_{cr} within the lifetime of the aircraft. The comparison results are given in Table 3, in which the 2nd row gives the number of total failures (for the case of no maintenance intervention) or the number of repaired panels (for the five maintenance strategies) over the entire fleet. The 3rd row presents the number of "unnecessary repaired" panels, i.e., panels that would not fail during the whole life but are nevertheless (unnecessarily) repaired according to the maintenance strategy. The 4th-6th rows give the minimal, the maximal and the average number of maintenance stops among the 100 aircraft, respectively. The number in the parentheses in the 6th row is the average number of unscheduled maintenance stops in CBM-skip and PdM-skip. Note that for CBM and PdM, all maintenances are unscheduled. The 7th-9th rows give the minimal, the maximal and the average number of repaired panels among the 100 aircraft. The last row gives the average cost of structural airframe maintenance over the 100 aircraft in each strategy.

It can be seen that if one lets cracks grow continuously without maintenance intervention, 692 panels over the whole fleet eventually fail. All these 692 panels are repaired in each maintenance strategy prior to their failure. In other words, all maintenance strategy can ensure safety. Each maintenance strategy has a different extent of "unnecessary repair". The number of unscheduled maintenances is zero in PdM-skip, which indicates that all maintenances occur at the times of scheduled maintenance and no unscheduled maintenance is asked. This does not mean that there will never be any but it is a rare event that we do not capture with our fleet size.

Table 3. Comparison of different processes

	No maintenance	Scheduled	CBM	CBM-skip	PdM	PdM-skip
Panels failed/repaired over the entire fleet	692	1403 repaired	1312 repaired	1238 repaired	789 repaired	798 repaired

	failures					
Unnecessary repairs	-	711	620	546	87	106
Minimal No. of maintenance stop	-	10	1	1	1	1
Maximal No. of maintenance stop	-	10	3	4	2	2
Avg. No. of maintenance stop	-	10	1.9	2.2 (0.06)	1.0	1.0 (0)
Minimal No. of repaired panels	-	5	2	3	2	2
Maximal No. of repaired panels	-	21	26	26	16	16
Avg. No. of repaired panels	-	14.03	13.12	12.38	7.89	7.98
Avg. cost of structural maintenance (M$)		17.9	8.92	5.50	4.88	3.05

The results of threshold-based maintenance strategies (i.e., scheduled maintenance, CBM and CBM-skip) shows that CBM and CBM-skip reduce the number of maintenance stops as well as the number of repaired panels compared to the traditional scheduled maintenance, thus reduce significantly the cost. CBM has fewer maintenance stops than CBM-skip (1.9 vs 2.2). However, since CBM is designed independently without taking into account the scheduled maintenance (Figure 5), all CBM stops are unscheduled maintenance and are more costly. In contrast, most of the maintenance stops of CBM-skip occur at the scheduled maintenance. Only very few unscheduled maintenance (0.06 on average) are required. In addition, CBM repairs slightly more panels than CBM-skip due to that CBM has a larger repair threshold ($a_{\text{rep-CBM}}$=4.8mm vs $a_{\text{rep-skip}}$=4mm). Therefore, CBM results in a higher maintenance cost than that of CBM-skip.

In order to analyze the gains of using prognostics-based maintenance strategies (PdM and PdM-skip), we first discuss the *conservativeness*. There are two different contributions to the conservativeness, the inter-aircraft variability and intra-aircraft variability. The first one refers to that the worst aircraft in the fleet may have a large crack size much sooner than the average, while the second one is related to different crack sizes and crack growth rates in one aircraft. The comparison of the unnecessary repairs allows comparing the conservativeness level of the various strategies.

Scheduled maintenance is clearly the most conservative since it needs to cover a very conservative crack size and crack growth rate both over the fleet and within an individual aircraft. In order to decrease the cost it makes sense to decrease the conservativeness level and the various maintenance strategies reduce the conservativeness to a different extent.

CBM and CBM-skip address the part that stems from inter-aircraft variability as well as the intra-aircraft variability related to different crack sizes, but it does not cover intra-aircraft variability related to different crack growth rates. Note that in order to quantify the conservativeness gains from CBM over the scheduled maintenance, we need to have a comparable number of maintenance stops, otherwise a higher number of maintenance stops would be traded off for a lower number of repaired panels. Accordingly, we set two stops for scheduled maintenance (closer to the number of stops in CBM 1.9) with a 20000 cycles interval, i.e., the first maintenance stop is at 20000th and the second is at 40000th cycle. In this case, the repair threshold decreases to a very small value 0.8e−3mm to maintain a reliability of 1e−7 in 20000 cycles for the entire fleet and the number of repaired panels goes up to 8990.

The conservativeness is further reduced by performing prognostics, which is the main point we want to make in this paper. Based on the prognostics method, we proposed two prognostics-based maintenance strategies (PdM and PdM-skip), both of which address the two contributions to the overall conservativeness, and thus decrease simultaneously the number of maintenance stops and repaired panels. On one hand, by setting a long "forward prediction interval" *h*, the average number of maintenance stops of the fleet in both PdM and PdM-skip reduce to nearly one. On the other hand, due to forecasting the crack growth trend, the number of unnecessary repaired panels is also significantly reduced compared to CBM and CBM-skip (reduction by more than an order of magnitude over CBM and CBM-skip). This is due to the fact that the proposed predictive maintenance takes into account the crack growth rate for each individual panel, while this could not be done in condition based approaches, which in terms allows to significantly reduce the number of unnecessary repairs. The reduction of both these aspects results in a considerable cost saving over CBM and CBM-skip, which shows the interest of using prognostics in the maintenance strategy.

Note that currently, the forward prediction interval is fixed as 23000 cycles for PdM and to the EOL (end of life) for PdM-skip (as a reference, in PdM-skip, the aircraft who demands the maintenance the earlies in the fleet is at 36000th cycle, therefore, the prediction interval for this aircraft is 24000 given that the lifetime of aircraft is 60000 flight cycles). On one hand, a long prediction interval tends to repair more panels at one stop, thus decreases the frequency of asking maintenance stop. In fact, we see from Table 3 that the average number of maintenance stop reduces to nearly one for both PdM and PdM-skip. On the other hand, the longer the forward prediction interval is, the more prediction uncertain will be involved, resulting in an increase of the number of repaired panels. In summary, a longer prediction interval will reduce the number of maintenance stops while increasing the number of repaired panels, and verse vice. For example, based on our experience, when the forward prediction interval in PdM-skip decreases to 4000, the average number of maintenance stops increases to 3.1 while the average number of

repaired panels decreases to 7.62 (i.e., 762 repaired panels for the whole fleet). Therefore, in reality, the number of maintenance stops and the number of repaired panels can be trade-off by tuning the prediction interval depending on the cost of one maintenance stop and the cost of repairing one panel. If the cost of one maintenance stop is much higher than that of repairing one panel, one would tend to repair more panels once a maintenance stop is triggered. In this case, it would be more meaningful to use a long prediction interval to trade off the number of repaired panels for the number of maintenance stops. In contrast, if the cost of repairing one panel is more significant than that of one maintenance stop, then a shorter prediction interval would make more sense.

We now discuss further the two prognostics-based strategies. PdM is designed completely independently without considering the time of maintenance schedule (Figure 5). All the stops are unscheduled maintenances that occurred out of the time of scheduled maintenance. In PdM-skip, all the maintenances are implemented during one of the 10 scheduled maintenance stops. The results indicate that PdM-skip fits well the objective that it ensures as much as possible that maintenance activities are carried out during the time of scheduled maintenance and this turns indeed out to be more economical from a maintenance cost point of view.

Figure 7-9 illustrate the statistical characters of the number of failed/repaired panels over the entire fleet, i.e., 100×500 panels. The histogram of the failure time in the case of no maintenance intervention is given in Figure 7. The numbers in the x-axis are the center of the bin and the bin width is 2000 cycles. For example, the first bin tells that the number of panels whose failure time is within the range of [36000, 38000] cycles is two. We see that most failures occur in the second half of the lifetime and the number of failed panels gradually increases toward the EOL (end of life).

Figure 8 compares the scheduled maintenance, CBM-skip and PdM-skip strategies in terms of the number of repaired panels at scheduled stops (reminder there are 10 scheduled stops, see Figure 5). The first three scheduled stops are not plotted because no panels are repaired at the first three stops in all strategies. It shows that PdM-skip reduces by nearly 80% the “unnecessary repair” compared to CBM-skip since PdM-skip decreases the conservativeness level by doing prognostics for each panel. The panels that are repaired in CBM-skip may not be necessary to be repaired in PdM-skip due to their slow growth rates, thus not threatening to safety. One may notice that PdM-skip repairs more panels than CBM-skip in the earlier stage of the aircraft lifetime. It is because once the maintenance is asked, PdM-skip performs a long horizon prediction. Therefore, the panels that might exceed the threshold in the later stage are repaired in advance. Once a panel is repaired, the crack is assumed to re-grow from a small initial crack size. The probability that this panel is repaired again during the aircraft lifetime is negligible.

Figure 9 compares CBM and PdM in terms of the number of repaired panels within the time range of each bin. The numbers in the x-axis are the center of the bin and the bin width is 2000 cycles. For example, the first bin means that there are two panels whose failure cycle is within the range of [36000, 38000] cycles for both CBM and PdM. It shows that PdM significantly reduces the number of repaired panels and the most of the panels are repaired at an earlier period of the aircraft lifetime due to a long forward

prediction interval. CBM repairs many cracks slightly larger than the repair threshold near the EOL but actually these panels do not affect safety. In contrast, PdM reduces these “unnecessary repair” by considering the future reliability.

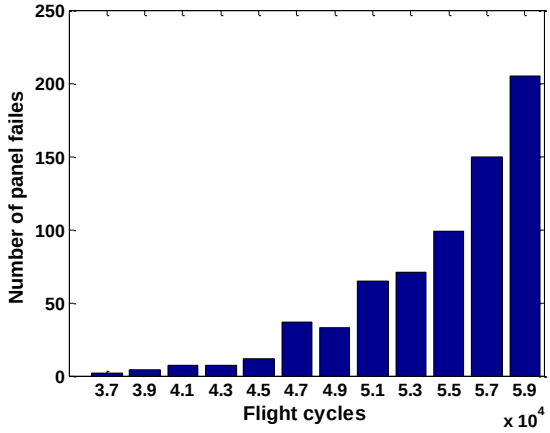

Figure 7. Number of panels fails within the range of each bin in the case of no maintenance process

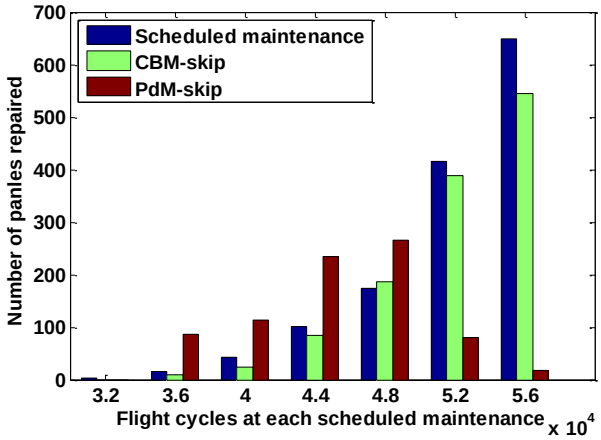

Figure 8. Comparison of maintenance strategies in terms of the number of repaired panels at scheduled maintenance stops. The first three scheduled stops are not plotted.

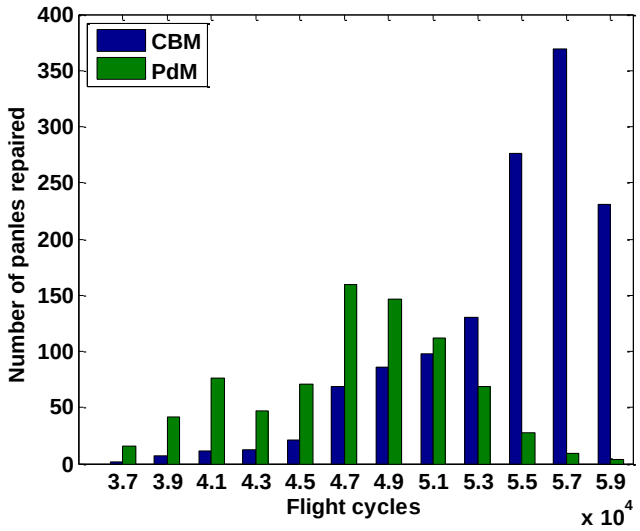

Figure 9. Comparison of CBM and PdM in terms of number of repaired panels within the time range of each bin

Figure 7-9 show the statistical behavior of the number of failed/repaired panels over the entire fleet. In order to give more insight into what happens in different processes, we take the simulation results of aircraft No.30 as an example and illustrate in Figure 10 which panels are repaired at which flight cycle in each process. The symbol "#" represents the panel index. The numbers in parentheses along the x-axis in subplots 1, 5 and 6 are the cycles corresponding to the failure/repair in the process of no maintenance intervention, CBM and PdM, respectively. For example, in subplot 1, the panel No.487 fails at 49600th cycle. The red solid dots and the green solid squares along y-axis represent the "real failed" panels and the "unnecessary repaired" panels, respectively. It can be seen that all the "real failed" panels shown in the first subplot are repaired in all other maintenance processes prior to their failure, that is to say, all maintenance strategies ensure safety. CBM wastes many panels near the EOL while PdM-skip and PdM have the least unnecessary repair.

In order to further assess the effectiveness of prognostics-based maintenance over threshold-based maintenance in different situations, we also studied the six maintenance strategies while considering a smaller panel-to-panel uncertainty, i.e., a smaller uncertainty on material properties $\{m,C\}$ and on the pressure differential p. This was implemented by reducing the coefficient of variance of $\{m,C\}$ and p in Table 2 to 0.5% while keeping other values unchanged. We found that prognostics-based strategies (PdM and PdM-skip) gain slightly over the threshold-based ones (CBM and CBM-skip) in terms of repaired panels in the small uncertainty case, while they more significantly outperform the threshold-based strategies when larger uncertainties are present. This is caused by the different philosophies of these two types of strategies. The prognostics-based strategies repair a panel based on its individual crack growth behavior while the threshold-based ones have the same repair threshold for all panels. Specifically, when the uncertainties on material property parameters $\{m,C\}$ and on pressure p are small, both the panel-to-panel variability and the variability presenting in the crack propagation process are small, leading the cracks in the panels to have similar propagation behavior. In this

situation, the two types of strategies have similar performance. In contrast, when large uncertainties are present on $\{m,C\}$ and p, the cracks have large variability in propagation rate among the panel population. In the threshold-based strategies, due to the constant repair threshold, all panels with a crack size greater than the repair threshold are repaired, even if some of them have a very low growth rate and are not likely to fail until the aircraft's end of life. Prognostics-based strategies have an advantage in this situation since they treat the panels individually. Combined with the crack size and the material property parameters of each panel at the current time, PdM/PdM-skip predict its crack growth trajectory in a future period and make the decision of whether or not replacing this panel based on this predicted behavior.

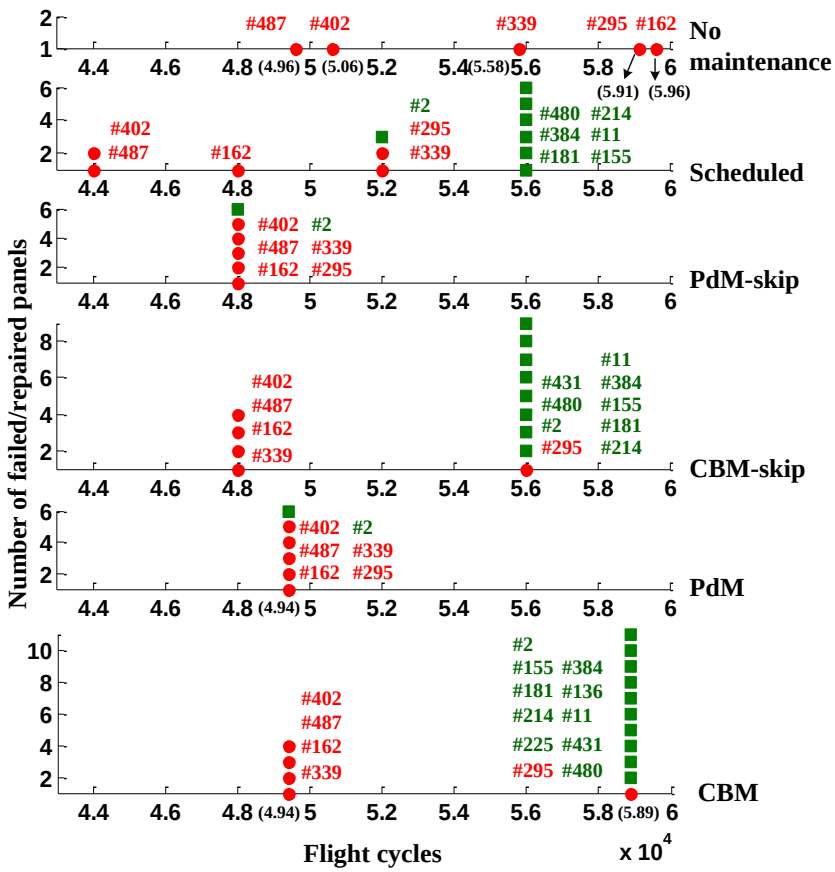

Figure 10. Different processes of aircraft #30

Conclusions

In the context of fatigue crack growth on fuselage panels, where the material properties and the initial crack sizes are unknown, and the cabin pressure differential is random, we proposed a model-based prognostics method and based on that proposed prognostics-based strategies (PdM/PdM-skip). PdM and PdM-skip are compared with the traditional scheduled maintenance and two other threshold-based strategies, i.e., CBM/CBM-skip proposed in Ref.[1], through applying on a fleet of short-range commercial aircraft. A cost model is used to quantify and compare the cost-effectiveness of different strategies. It is

found that PdM/PdM-skip gain significantly over scheduled maintenance and CBM/CBM-skip because the reliability in the future is calculated individually for each panel and this predicted reliability is incorporated into maintenance decision-making. As for the comparison between the two prognostics-based strategies, all maintenance stops incurred by PdM occur as unscheduled maintenance, which is more expensive due to less advance notice, while almost all maintenance stops incurred by PdM-skip happen at scheduled maintenance.

However, due to the Gaussian assumption of the EKF, the crack size is assumed normally distributed throughout all the stages, which may not be sufficient, once real measurements will be available. This assumption could be relaxed by choosing some non-Gaussian filter methods instead of the EKF. Accordingly, the FOP method could also be extended to adapt to the non-Gaussian assumption on crack size distribution. In addition, in the cost model, the interaction between the cost of repairing one panel at scheduled maintenance and the one at unscheduled maintenance is not considered, which might affect the maintenance cost of different strategies. For example, if the cost of unscheduled repair is much higher than the scheduled repair, the decision maker might prefer to repair as many panels as possible at scheduled maintenance to avoid unscheduled maintenance. In contrast, if the unscheduled repair is not much higher than, or even close to the scheduled repair, then it might not be necessary to make a trade-off between scheduled and unscheduled repair. That is to say, the cost ratio of scheduled repair to unscheduled repair could affect the maintenance decision-making. Future work will consider different cost ratios and develop an optimal maintenance strategy that minimizes the maintenance cost for a given time horizon.

Appendix 1

Model the degradation process as a Hidden Markov model

The Euler method is used to solve the differential equation of Eq.(1) with a discrete step size of one. The discrete Paris model is written in a recursive form given in Eq.(7).

$$\begin{aligned} a_k &= a_{k-1} + C\left(A\frac{p_{k-1}r}{t}\sqrt{\pi a_{k-1}} \right)^m \\ &= g(a_{k-1}, p_{k-1}) \end{aligned} \tag{7}$$

We model the pressure differential p as a random variable that varies at every flight cycle. At cycle k, p is modeled as

$$p_k = \bar{p} + \Delta p_k \tag{8}$$

where $\bar{p}$ is the average pressure differential and Δp_k is the pressure disturbance. The disturbance around the average pressure is modeled as a random variable that is normally distributed with zero mean and variance σ_p^2. Since uncertainty in pressure differential is

generally small, a Mean-Value First Order Second Moment (MVFOSM) approach [37] is used here. Then Eq.(7) can be written as:

$$a_k = g(a_{k-1}, \overline{p}) + \frac{\partial g(a_{k-1}, \overline{p})}{\partial p} \Delta p_{k-1} \tag{9}$$

in which $(\partial g(a_{k-1}, \overline{p}) / \partial p)\Delta p_{k-1}$ is seen as the additive process noise. By considering that $\overline{p}$ is a constant, Eq.(9) becomes:

$$a_k = f(a_{k-1}) + w_{k-1} \tag{10}$$

where $f(a_{k-1}) = g(a_{k-1}, \overline{p})$ and

$$w_{k-1} = (\partial f(a_{k-1}) / \partial p)\Delta p_{k-1} \tag{11}$$

Given that Δp_{k-1} is normally distributed and $\partial f(a_{k-1}) / \partial p$ is constant, the additive process noise w_k follows a normal distribution with mean zero and variance Q_k, which is calculated analytically by Eq.(12).

$$\begin{aligned} Q_k &= \left(\frac{\partial g(a_k, \overline{p})}{\partial p} \sigma_p \right)^2 \\ &= \left(Cm(Ar/t)^m (\overline{p})^{m-1} (\pi a_k)^{m/2} \sigma_p \right)^2 \end{aligned} \tag{12}$$

The noisy measurement data is simulated using Eq.(13), in which a_k is the crack size at k-th cycle and v_k the measurement noise.

$$z_k = a_k + v_k \tag{13}$$

Eq.(10) and Eq.(13) are the state equation and the measurement equation of the Hidden Markov model, respectively.

In terms of state-parameter estimation using EKF, it defines the parameter vector as an additional state variable and artificially appends it onto the true state vector to form a single joint state vector and estimate the state and parameters simultaneously. In the aforementioned crack growth model, m and C are the unknown parameters that need to be estimated. Therefore, a two-dimensional parameter vector is defined as

$$\Theta = [m, C]^T \tag{14}$$

Appending Θ to the state variable, the augmented state vector is then defined in Eq.(15).

$$\boldsymbol{x}_{\text{au}} = [a\ m\ C]^T \tag{15}$$

The EKF is used as a black box and the detail of the algorithm will not be presented here. Readers could refer to Ref. [38, 39] for a general introduction and to Ref. [40] for its implementation to fatigue damage state estimation. By applying EKF, at cycle k, the a posteriori estimation of the augmented state vector, denoted by $\boldsymbol{x}_{\mathrm{au},k}$, and the corresponding covariance matrix $\boldsymbol{P}_k$ can be obtained.

Details of First-Order Perturbation method

Suppose the current flight cycle is S. According to the EKF, the state vector $\boldsymbol{x}_{\mathrm{au},S}$ is multivariate normally distributed with mean $\hat{\boldsymbol{x}}_{\mathrm{au},S}$ and covariance $\boldsymbol{P}_S$, presented as

$$\boldsymbol{x}_{\mathrm{au},S} \sim N(\hat{\boldsymbol{x}}_{\mathrm{au},S}, \boldsymbol{P}_S) \tag{16}$$

Let us define:

$$f_{\mathrm{L}}(a, m, C, p) = C(A\frac{pr}{t}\sqrt{\pi a})^m \tag{17}$$

The Paris model is then written as

$$a_k = a_{k-1} + f_{\mathrm{L}}(a_{k-1}, m, C, p_{k-1}) \tag{18}$$

Note that the time index k starts from S+1 and goes up to S+h, where h is the time span that how many flight cycles forward one want to predict. In the stochastic process, the "expected trajectory" is the particular solution when the involved random variables are taken their expected values. For the problem discussed at hand, the "expected trajectory" of the crack size is the sequence $\{\bar{a}_k | k = S+1, S+2, ..., S+h\}$ obtained as a solution of the equation Eq.(19), with zero process noise and with the expected value $\bar{a}_S$, $\bar{m}$, $\bar{C}$ and $\bar{p}$ as the initial values of the corresponding random variables. Note that the symbol "–" is to denote the expected value of a random variable.

$$\bar{a}_k = \bar{a}_{k-1} + f_{\mathrm{L}}(\bar{a}_{k-1}, \bar{m}, \bar{C}, \bar{p}) \tag{19}$$

Due to the presence of uncertainties and the random noise, a_k, m, C and p_k are modeled by adding a perturbation from their expected values. Let the symbol "Δ" denotes the perturbation, the real a_k, m, C and p_k can be written as

$$a_k = \bar{a}_k + \Delta a_k \tag{20}$$
$$m = \bar{m} + \Delta m \tag{21}$$
$$C = \bar{C} + \Delta C \tag{22}$$
$$p_k = \bar{p} + \Delta p_k \tag{23}$$

Δp_k is related to the cabin pressure differential that varies from cycle to cycle while Δm and ΔC are uncertainties related to panel materials and thus do not vary with

time. The available information at $k=S$, as given in Eq.(24) and Eq.(25), will be used as the initial condition in the following derivation.

$$\left[\bar{a}_S, \bar{m}, \bar{C}\right]^{\mathrm{T}} = \left[\hat{a}_S, \hat{m}_S, \hat{C}_S\right]^{\mathrm{T}} \tag{24}$$

$$\left[\Delta a_S, \Delta m, \Delta C\right]^{\mathbf{T}} \sim N(\mathbf{0}_{3\times1}, \boldsymbol{P}_S) \tag{25}$$

By subtracting Eq.(19) from Eq.(18), the perturbation of a_k is obtained as

$$\Delta a_k = \Delta a_{k-1} + f_{\mathrm{L}}(a_{k-1}, m, C, p_{k-1}) - f_{\mathrm{L}}(\bar{a}_{k-1}, \bar{m}, \bar{C}, \bar{p}) \tag{26}$$

The first order approximation is used. Defining $\boldsymbol{\lambda}_{k-1} = [\bar{a}_{k-1}, \bar{m}, \bar{C}, \bar{p}]$, which is a known vector, Eq.(26) reduces to

$$\Delta a_k = \Delta a_{k-1} + \frac{\partial f_{\mathrm{L}}(\boldsymbol{\lambda}_{k-1})}{\partial a}\Delta a_{k-1} + \frac{\partial f_{\mathrm{L}}(\boldsymbol{\lambda}_{k-1})}{\partial m} + \frac{\partial f_{\mathrm{L}}(\boldsymbol{\lambda}_{k-1})}{\partial C}\Delta C + \frac{\partial f_{\mathrm{L}}(\boldsymbol{\lambda}_{k-1})}{\partial p}\Delta p_{k-1} \tag{27}$$

The following substitution is done to make the Eq.(27) simpler.

$$L_{k-1} = 1 + \frac{\partial f_{\mathrm{L}}(\boldsymbol{\lambda}_{k-1})}{\partial a} \tag{28}$$

$$M_{k-1} = \frac{\partial f_{\mathrm{L}}(\boldsymbol{\lambda}_{k-1})}{\partial m} \tag{29}$$

$$N_{k-1} = \frac{\partial f_{\mathrm{L}}(\boldsymbol{\lambda}_{k-1})}{\partial C} \tag{30}$$

$$w_{k-1}^{\mathrm{L}} = \frac{\partial f_{\mathrm{L}}(\boldsymbol{\lambda}_{k-1})}{\partial p}\Delta p_{k-1} \tag{31}$$

in which w_{k-1}^{L} is the random noise with mean zero and standard deviation $\sigma_{k\text{-}1}$, which can be calculated by Eq.(32). Here w_i^{L} and w_j^{L} ($i \neq j$) are considered independent.

$$\sigma_{k-1} = \frac{\partial f(\boldsymbol{\lambda}_{k-1})}{\partial p}\sigma_{\mathrm{p}} \tag{32}$$

Then Eq.(27) becomes

$$\Delta a_k = L_{k-1}\Delta a_{k-1} + M_{k-1}\Delta m + N_{k-1}\Delta C + w_{k-1}^{\mathrm{L}} \tag{33}$$

The following derivation is to calculate the uncertainty structure of Δa_k. Rewrite Eq.(33) as the function of the initial value, i.e., [Δa_S Δm, ΔC], then after k times iteration, Δa_k can be written as Eq.(34), in which we use A_k, B_k and D_k to represent the coefficient of Δa_S, Δm and ΔC respectively and E_k to denotes the noise term.

$$\Delta a_k = A_k \Delta a_S + B_k \Delta m + D_k \Delta C + E_k \tag{34}$$

In Eq.(34), Δa_S, Δm and ΔC are stationary random variables whose probability distributions do not change when shifted in time. A_k, B_k and D_k are deterministic and evolve with time, which are calculated recursively with their initial values A_S, B_S, C_S, as shown in Eqs.(35)-(37). E_k is a non-stationary random variable whose distribution varies with time and is derived recursively by Eq.(38). Given that E_k is a linear combination of independent and identically distributed variables, it is a normal variable such that $E_k \sim N(0, F_k)$. F_k is calculated by the recursive expression given in Eq.(39). Note that w_k^L and σ_k in Eq.(38) and Eq.(39) refer to Eq.(31) and Eq.(32), respectively.

$$A_k = L_k A_{k-1} \tag{35}$$
$$B_k = L_k B_{k-1} + M_k \tag{36}$$
$$D_k = L_k D_{k-1} + N_k \tag{37}$$
$$E_k = L_k E_{k-1} + w_k^{\mathrm{L}} \tag{38}$$
$$F_k = L_k^2 F_{k-1} + \sigma_k^2 \tag{39}$$

Provided that Δa_S, Δm, ΔC and E_k are random variables and that A_k B_k D_k are deterministic, Eq.(34) is rewritten as matrix form such that $\Delta a_k = \boldsymbol{B}_k \boldsymbol{\beta}_k$, in which $\boldsymbol{B}_k = [A_k, B_k, D_k, 1]$ and $\boldsymbol{\beta}_k = [\Delta a_S, \Delta m, \Delta C, E_k]^{\mathrm{T}}$. Considering $[\Delta a_S, \Delta m, \Delta C]^{\mathrm{T}} \sim N(\mathbf{0}_{3\times1}, \boldsymbol{P}_S)$ and $E_k \sim N(0, F_k)$, $\boldsymbol{\beta}_k$ is a multivariate normal vector such that $\boldsymbol{\beta}_k \sim N(\boldsymbol{\mu}, \boldsymbol{\Sigma})$, in which $\boldsymbol{\mu} = [\mathbf{0}_{4\times1}]$ and $\boldsymbol{\Sigma} = \mathrm{diag}(\boldsymbol{P}_S, F_k)$. According to the theory of affine transformation of multivariate Gaussian random variables, Δa_k is normally distributed such that $\Delta a_k \sim N(\boldsymbol{B}_k \boldsymbol{\mu}, \boldsymbol{B}_k \boldsymbol{\Sigma} \boldsymbol{B}_k^{\mathrm{T}})$, in which

$$\boldsymbol{B}_k \boldsymbol{\mu} = 0 \tag{40}$$
$$\boldsymbol{B}_k \boldsymbol{\Sigma} \boldsymbol{B}_k^{\mathrm{T}} = [A_k, B_k, D_k] \boldsymbol{P}_S [A_k, B_k, D_k]^{\mathrm{T}} + F_k \tag{41}$$

Given that $a_k = \bar{a}_k + \Delta a_k$ and $\bar{a}_k$ is deterministic, a_k is a normal variable that $a_k \sim N(\mu_{ak}, \sigma_{ak})$, in which

$$\mu_{ak}^{\mathrm{F}} = \bar{a}_k \tag{42}$$
$$\sigma_{ak}^{\mathrm{F}} = \sqrt{\boldsymbol{B}_k \boldsymbol{\Sigma} \boldsymbol{B}_k^{\mathrm{T}}} \tag{43}$$

The superscript "F" stands for FOP method in order to distinguish the Monte Carlo simulation that will be presented in Appendix 2. Eq.(42) and Eq.(43) enable to compute analytically the crack size distribution from cycle $S+1$ to cycle $S+h$.

Appendix 2 Performance comparison between FOP method and Monte Carlo simulation

We verify the accuracy of the proposed FOP method by comparing it with Monte Carlo (MC) simulation. According to the subsection "Results and discussions", if no maintenance process is carried out, there are 692 failed panels, i.e., the crack sizes on these 692 panels exceed the critical threshold a_{cr} before the end of the aircraft lifetime (60000 cycles). Failed panels imply faster crack growth rates and stronger nonlinear crack growth curves. In contrast, the non-failed panels indicate that the cracks maintain a moderate or very low growth rate and thus the crack growth curves show "minor nonlinearity" during the whole lifetime of the aircraft. If the FOP method performs well in the strong nonlinear crack growth process (corresponding to the failed panels), then it also maintains reasonably good efficacy for the minor nonlinear cases (non-failed panels). Therefore, we investigate the accuracy of the FOP method on the failed panels. Due to the limitations of space, we chose randomly 10 panels from the 692 failed panels to present the results quantitatively.

The initial conditions of each of these 10 panels, i.e., the initial crack size, the true Paris model parameters m and C are reported in Table 4. The last column is the service life of each panel. It is noted that that the service life of one panel is the accumulated flight cycles of the panel right before the crack size exceeding the critical threshold a_{cr}=59.6mm. The service life of the i-th panel is denoted by L^i.

Table 4 Initial condition of the 10 picked panels

No.	a_0 (mm)	m	C	Corresponding service life (cycles)
1	0.45	3.8	1.87E-10	52700
2	0.61	3.7	1.95E-10	51300
3	0.58	3.8	1.86E-10	45000
4	0.44	3.7	1.98E-10	59300
5	0.61	3.7	1.92E-10	46700
6	0.59	3.6	2.03E-10	58700
7	0.46	3.8	1.86E-10	58800
8	0.54	3.7	1.98E-10	57600
9	0.47	3.7	1.90E-10	59400
10	0.50	3.7	1.96E-10	57300

For each of the critical panels, we predict the evolution of the crack size distribution by using FOP method and MC simulation in the last J cycles prior to the end

of the service life of each panel. This allows to validate the FOP method since we deal with the most non-linear part of the crack growth curve. If the FOP method performs well in the most nonlinear stage, then it maintains reasonably good efficacy for the minor nonlinear stage. An example is taken here. The service life of panel No.1 in Table 4 is 52700 cycles. The EKF is applied from the first cycle up to the 46723th cycles (50723-4000=46723) to get the estimates of model parameters and crack size. Then the FOP method and the MC simulation are carried out to predict respectively the evolution of the crack size distribution from 46724th cycle to 50723th cycle. The evolution of the distribution given by FOP is compared with that given by MC simulation to investigate the performance of FOP method. The details for implementing the comparison are elaborated below:

Step 1 - For the i-th panel (i=1,2,…,10), apply the EKF to carry out the state-parameter estimation from cycle k=1 until $k=L^i-J$. The estimated state vector and the covariance matrix at $k=L^i-J$ are denoted as $\hat{\boldsymbol{x}}_{\mathrm{au},L^i-J}$ and $\boldsymbol{P}_{L^i-J}$.

Step 2 - From $k=L^i-J+1$ to $k=L^i$ (i.e., the last J cycles), predict the mean μ_{ak}^{F} (see Eq.(42)) and standard deviation σ_{ak}^{F} (see Eq.(43)) of the crack size using FOP method (see Appendix 1 for details).

Step 3 - From $k=L^i-J+1$ to $k=L^i$ (i.e., the last J cycles), predict the mean and the standard deviation of the crack size using MC simulation. Specifically, generate N_{s} samples at $k=L^i-J$ based on $\hat{\boldsymbol{x}}_{\mathrm{au},L^i-J}$ and $\boldsymbol{P}_{L^i-J}$, i.e. sample $\boldsymbol{x}^j_{\mathrm{au},L^i-J}\sim N(\hat{\boldsymbol{x}}_{\mathrm{au},L^i-J},\boldsymbol{P}_{L^i-J})$ (j=1,2,…N_{s}). Propagate forward each sample from $k=L^i-J+1$ to $k=L^i$ through Eq.(10) and then at cycle k, the mean and standard deviation, denoted by μ_{ak}^{M} and σ_{ak}^{M}, can be calculated from the N_{s} samples.

According to the nature of the EKF-FOP method, the crack size is normally distributed characterized by mean and standard deviation. Therefore, comparing the crack size distribution predicted by FOP and MC methods is equivalent to comparing μ_{ak}^{F} and μ_{ak}^{M}, σ_{ak}^{F} and σ_{ak}^{M} ($k=L^i-J+1$, L^i-J+2, …, L^i).

The relative error between μ_{ak}^{F} and μ_{ak}^{M}, σ_{ak}^{F} and σ_{ak}^{M} are calculated as follows, $e_{\mu k}=|\mu_{ak}^{\mathrm{F}}-\mu_{ak}^{\mathrm{M}}|/\mu_{ak}^{M}$, $e_{\sigma k}=|\sigma_{ak}^{\mathrm{F}}-\sigma_{ak}^{\mathrm{M}}|/\sigma_{ak}^{\mathrm{M}}$, ($k=L^i-J+1$, L^i-J+2, …, L^i). The relative error increases as cycles increase. We present in Table 5 the maximum value of $e_{\mu k}$ and $e_{\sigma k}$, which are obtained at the end of the service life ($k=L^i$) of each panel. The first column is the index of the panel whose initial condition and the corresponding service life have been presented in Table 4. One may note that the true crack size at the end of the service life of each panel is smaller than the critical threshold a_{cr}=59.6mm. That is because the crack size grows very fast in the stage near the threshold and exceeds a_{cr} in the next maintenance assessment interval (100 cycles).

Table 5 Comparison of the mean and standard deviation of the crack size given by FOP and MC simulation at the end of the service life ($k=L^i$) of each panel

No.	μ_{ak}^{F}	μ_{ak}^{M}	$e_{\mu k}$ (%)	σ_{ak}^{F}	σ_{ak}^{M}	$e_{\sigma k}$ (%)	True crack	95% C.I. based on

	(mm)	(mm)		(mm)	(mm)		size (mm)	μ_{ak}^{F} and σ_{ak}^{F} (mm)
1	58.08	58.83	1.26	7.75	8.03	3.51	55.94	[42.89, 73.28]
2	60.00	60.19	0.31	4.42	4.55	2.76	58.50	[51.33, 68.67]
3	62.68	63.29	0.96	7.88	8.13	3.14	56.65	[47.25, 78.12]
4	56.02	56.30	0.49	5.29	5.30	0.11	54.78	[45.65, 66.39]
5	54.96	55.20	0.42	4.66	4.81	3.01	53.91	[45.83, 64.10]
6	59.26	59.39	0.22	3.37	3.44	2.05	59.18	[52.66, 65.86]
7	60.13	60.55	0.69	6.08	6.27	3.01	59.57	[48.22, 72.04]
8	55.68	55.78	0.18	3.71	3.74	0.78	55.74	[48.41, 62.95]
9	54.09	54.23	0.26	4.59	4.65	1.17	54.19	[45.09, 63.08]
10	56.48	56.57	0.16	4.77	4.85	1.66	56.62	[47.12, 65.83]

We draw the following conclusions based on the results. (1). The FOP method gives very close results to that of MC with maximal relative error 1.26% for the mean (panel No.1) and 3.51% for the standard deviation (panel No.1). (2) For panels Nos. 8, 9 and 10, the mean of the crack size estimated by FOP is a bit underestimated (i.e., smaller than the true crack size). However, when considering the 95% confidence interval, the prediction remains conservative. The last column presents all the 95% confidence interval of the predicted mean. (3) The FOP method shows its great advantage in computational cost over MC (5000 samples are used). The processing time of predicting one crack growth in one panel is 0.006s (FOP) vs 29s (MC) on a laptop with a processor Intel (R) Core(TM) i5-3337U CPU 1.8GHz. This computational saving is significantly meaningful to the predictive maintenance proposed in this paper since the maintenance strategies are applied in an aircraft fleet containing thousands of panels.

Appendix 3 Evaluating the prognostics method by prognostics metrics

The proposed prognostics method is further evaluated by comparing with true known remaining useful life (RUL) using five established prognostics metrics[30]: prognostics horizon (PH), $\alpha-\lambda$ accuracy, relative accuracy (RA), cumulative relative accuracy (CRA), and convergence. Readers refer to Ref.[30, 33] for detail information about the five metrics. It is noted that these metrics are possible only when the true RUL is available.

We continue to use the ten panels that were randomly picked from the 692 failed panels in Appendix 2 to verify the proposed prognostics method. The service life of each

panel is listed in Table 4, which is used to obtain the true RUL. The predicted RUL is computed each time when a new measurement arrives and the state-parameter is carried out by the EKF until the end of the service life of the panel.

The PH, $\alpha - \lambda$ accuracy, RA, CRA and convergence of the ten panels are reported in Table 6. For PH and $\alpha - \lambda$ accuracy, $\alpha = 0.1$, $\lambda = 0.5$ are used. A larger PH indicates a better performance, which allows earlier prediction for the end of service life with more reliability. RA equals to one minus the relative error between the true RUL and the predicted one at a specific cycle, while CRA is the same as the average of RA values accumulated at every cycle. Therefore, for RA and CRA, the closer to one, the higher the relative accuracy is. As for convergence, the smaller the value is, the faster the convergence is. From Table 6, we see that for all the ten panels, the proposed prognostics method gives a large PH, high value of RA and CRA, and a relatively small value of convergence compared to their service lives. Therefore, the proposed prognostics method performs satisfactorily.

For illustration purposes we provide the plots of the PH and $\alpha - \lambda$ accuracy for panels Nos.1-4, as shown in Figure 11 and Figure 12, respectively.

Table 6 The five metrics for the ten panels

Panel No.	PH(α=0.1)	$\alpha - \lambda$ accuracy (α=0.1, $\lambda = 0.5$)	RA	CRA	Convergence
No.1	52500	True	0.93	0.97	21248
No.2	47500	False	0.99	0.98	9445
No.3	38100	True	0.94	0.94	11096
No.4	49900	True	0.96	0.93	13936
No.5	37800	True	0.99	0.93	12618
No.6	50700	False	0.95	0.86	8894
No.7	51900	False	0.95	0.92	10703
No.8	43400	False	0.98	0.93	14592
No.9	48700	False	0.97	0.91	11355
No.10	46500	False	0.93	0.86	11388

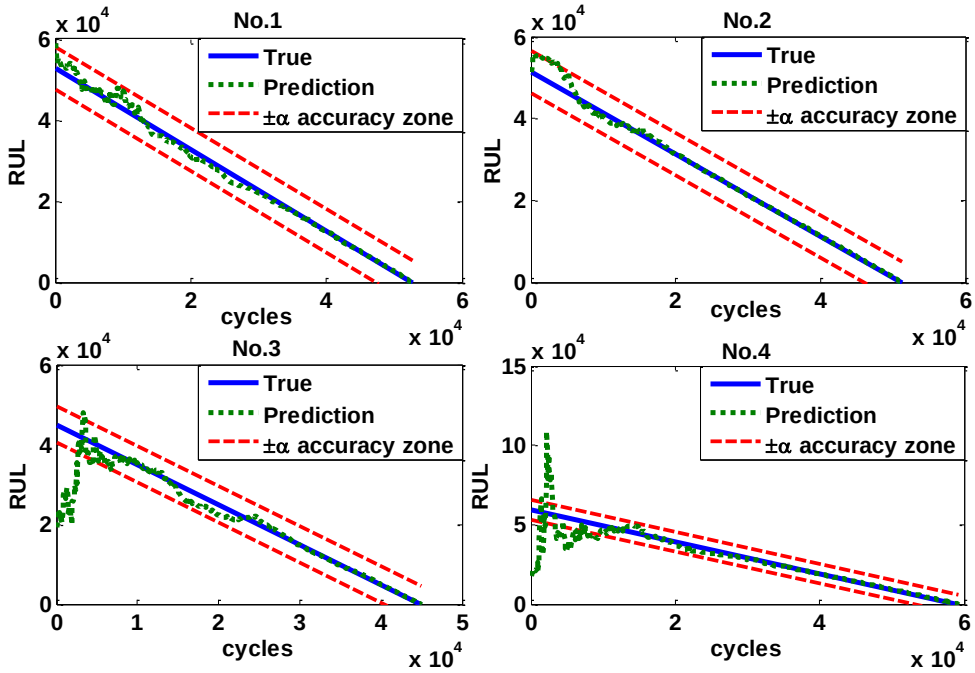

Figure 11 PH with $\alpha = 0.1$ of panels Nos.1-4

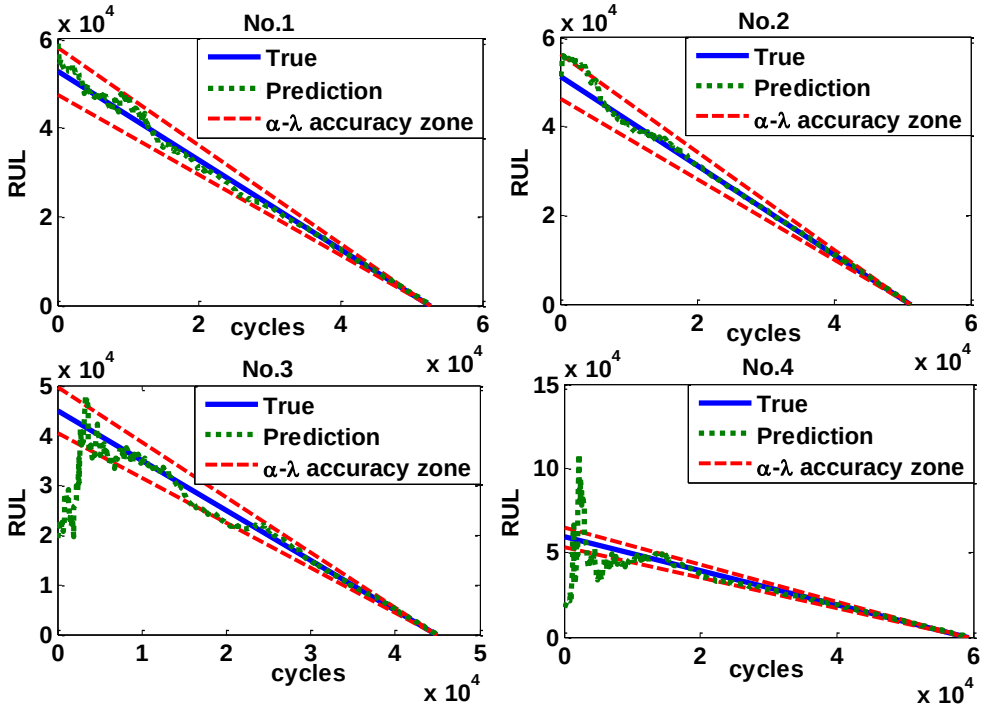

Figure 12 $\alpha - \lambda$ accuracy with $\alpha = 0.1$ and $\lambda = 0.5$ of panels Nos.1-4

Appendix 4 Details of CBM and CBM-skip strategies

The SHM system is assumed to be used in CBM and CBM-skip and damage assessment is done every 100 flights. In CBM, at each damage assessment, if the largest crack size in

an aircraft exceeds a_{maint}, unscheduled maintenance is trigged immediately without considering the scheduled maintenance (Figure 5), i.e., the maintenance could occur anytime unexpectedly, outside of the 10 scheduled maintenance stops. Once unscheduled maintenance is requested, all the panels with a crack size larger than a repair threshold $a_{rep\text{-}CBM}$ are repaired. Figure 13 illustrates a flowchart of CBM.

In contrast, CBM-skip takes into account the scheduled maintenance but aims at skipping some unnecessary early scheduled maintenance. The flowchart of CBM-skip is shown in Figure 14. At each scheduled maintenance stop, if there is no crack exceeding a threshold $a_{th\text{-}skip}$, then the current scheduled maintenance is skipped. Note that $a_{th\text{-}skip}$ can be much less conservative than the repair threshold in scheduled maintenance since damage assessment is also carried out very frequently outside of the scheduled maintenance stops. If there is a crack, which grows beyond a_{maint} between two consecutive scheduled maintenance stops then an unscheduled maintenance is trigged at once and all panels with crack size greater than $a_{rep\text{-}skip}$ are repaired.

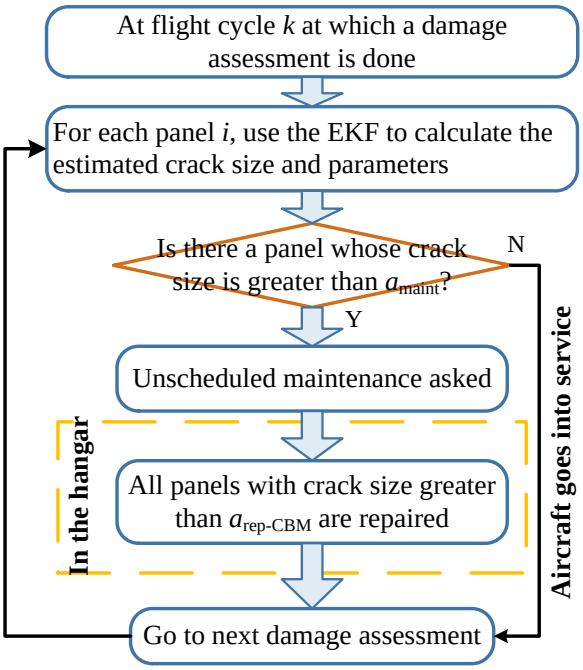

Figure 13. Flowchart of CBM

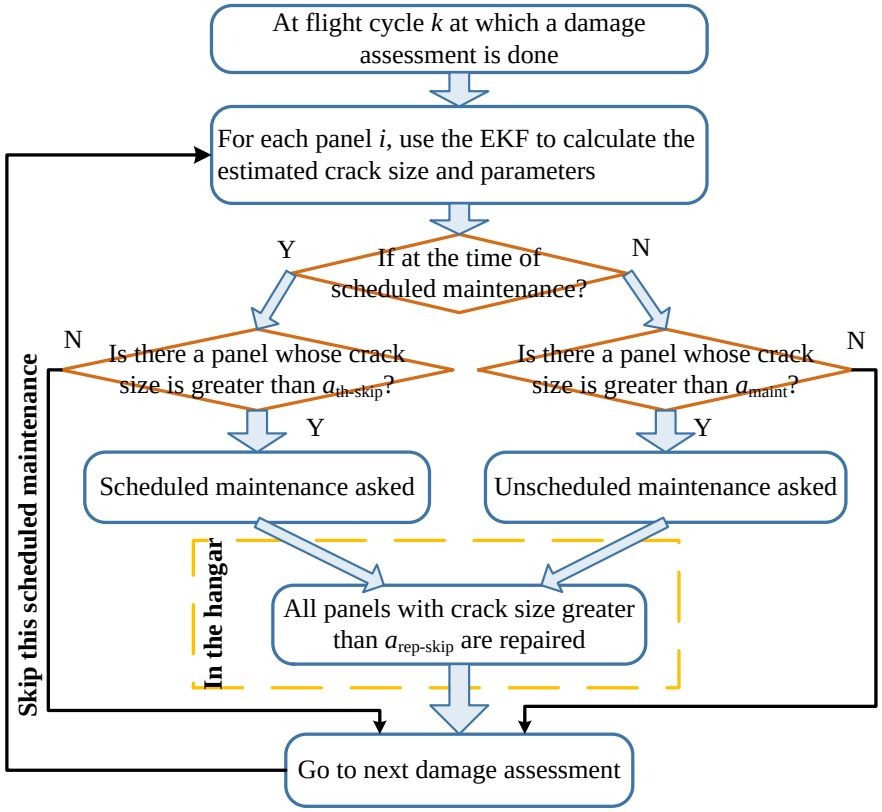

Figure 14. Flowchart of CBM-skip

References

1. Pattabhiraman S, Gogu C, Kim NH, Haftka RT, Bes C. Skipping unnecessary structural airframe maintenance using an on-board structural health monitoring system. *Proceedings of the Institution of Mechanical Engineers, Part O: Journal of Risk and Reliability*. 2012; 226: 549-60.
2. Xiaoliang Z, Huidong G, Guangfan Z, et al. Active health monitoring of an aircraft wing with embedded piezoelectric sensor/actuator network: I. Defect detection, localization and growth monitoring. *Smart Materials and Structures*. 2007; 16: 1208.
3. Ignatovich SR, Menou A, Karuskevich MV, Maruschak PO. Fatigue damage and sensor development for aircraft structural health monitoring. *Theoretical and Applied Fracture Mechanics*. 2013; 65: 23-7.

4. Diamanti K, Soutis C. Structural health monitoring techniques for aircraft composite structures. *Progress in Aerospace Sciences*. 2010; 46: 342-52.
5. Jeong-Beom I, Fu-Kuo C. Detection and monitoring of hidden fatigue crack growth using a built-in piezoelectric sensor/actuator network: I. Diagnostics. *Smart Materials and Structures*. 2004; 13: 609.
6. Deloux E, Castanier B, Bérenguer C. Maintenance policy for a deteriorating system evolving in a stressful environment. *Proceedings of the Institution of Mechanical Engineers, Part O: Journal of Risk and Reliability*. 2008; 222: 613-22.
7. Huynh KT, Barros A, Berenguer C. Adaptive condition-based maintenance decision framework for deteriorating systems operating under variable environment and uncertain condition monitoring. *Proceedings of the Institution of Mechanical Engineers, Part O: Journal of Risk and Reliability*. 2012; 226: 602-23.
8. Wang W, Hussin B, Jefferis T. A case study of condition based maintenance modelling based upon the oil analysis data of marine diesel engines using stochastic filtering. *International Journal of Production Economics*. 2012; 136: 84-92.
9. Wang HK, Huang HZ, Li YF, Yang YJ. Condition-Based Maintenance With Scheduling Threshold and Maintenance Threshold. *IEEE Transactions on Reliability*. 2016; 65: 513-24.
10. Huynh KT, Barros A, Berenguer C. Multi-Level Decision-Making for The Predictive Maintenance of k-out-of-n: F deteriorating systems. *IEEE Transactions on Reliability*. 2015; 64: 94-117.
11. Huynh KT, Barros A, Berenguer C. Maintenance Decision-Making for Systems Operating Under Indirect Condition Monitoring: Value of Online Information and Impact of Measurement Uncertainty. *IEEE Transactions on Reliability*. 2012; 61: 410-25.

12. Deloux E, Castanier B, Bérenguer C. Predictive maintenance policy for a gradually deteriorating system subject to stress. *Reliability Engineering & System Safety*. 2009; 94: 418-31.
13. Curcurù G, Galante G, Lombardo A. A predictive maintenance policy with imperfect monitoring. *Reliability Engineering & System Safety*. 2010; 95: 989-97.
14. Van Horenbeek A, Pintelon L. A dynamic predictive maintenance policy for complex multi-component systems. *Reliability Engineering & System Safety*. 2013; 120: 39-50.
15. Nguyen K-A, Do P, Grall A. Multi-level predictive maintenance for multi-component systems. *Reliability Engineering & System Safety*. 2015; 144: 83-94.
16. Lorton A, Fouladirad M, Grall A. Computation of remaining useful life on a physic-based model and impact of a prognosis on the maintenance process. *Proceedings of the Institution of Mechanical Engineers, Part O: Journal of Risk and Reliability*. 2013; 227: 434-49.
17. Langeron Y, Grall A, Barros A. A modeling framework for deteriorating control system and predictive maintenance of actuators. *Reliability Engineering & System Safety*. 2015; 140: 22-36.
18. Liu J, Zhang M, Zuo H, Xie J. Remaining useful life prognostics for aeroengine based on superstatistics and information fusion. *Chinese Journal of Aeronautics*. 2014; 27: 1086-96.
19. Jardine AKS, Lin D, Banjevic D. A review on machinery diagnostics and prognostics implementing condition-based maintenance. *Mechanical Systems and Signal Processing*. 2006; 20: 1483-510.
20. Wang Y, Gogu C, Binaud N, Bes C, Haftka RT, Kim NH. A cost driven predictive maintenance policy for structural airframe maintenance. *Chinese Journal of Aeronautics*.
21. Paris P, Erdogan F. A Critical Analysis of Crack Propagation Laws. *Journal of Basic Engineering*. 1963; 85: 528-33.

22. Tanaka K, Masuda C, Nishijima S. The generalized relationship between the parameters C and m of Paris' law for fatigue crack growth. *Scripta Metallurgica*. 1981; 15: 259-64.
23. Molent L, Barter SA. A comparison of crack growth behaviour in several full-scale airframe fatigue tests. *International Journal of Fatigue*. 2007; 29: 1090-9.
24. Karandikar JM, Kim NH, Schmitz TL. Prediction of remaining useful life for fatigue-damaged structures using Bayesian inference. *Engineering Fracture Mechanics*. 2012; 96: 588-605.
25. Gobbato M, Kosmatka JB, Conte JP. A recursive Bayesian approach for fatigue damage prognosis: An experimental validation at the reliability component level. *Mechanical Systems and Signal Processing*. 2014; 45: 448-67.
26. Sun J, Zuo H, Wang W, Pecht MG. Prognostics uncertainty reduction by fusing on-line monitoring data based on a state-space-based degradation model. *Mechanical Systems and Signal Processing*. 2014; 45: 396-407.
27. Doucet A, Johansen AM. A tutorial on particle filtering and smoothing: Fifteen years later. *Handbook of nonlinear filtering*. 2009; 12: 656-704.
28. Roblès B, Avila M, Duculty F, Vrignat P, Bégot S, Kratz F. Hidden Markov model framework for industrial maintenance activities. *Proceedings of the Institution of Mechanical Engineers, Part O: Journal of Risk and Reliability*. 2014; 228: 230-42.
29. Le TT, Chatelain F, Bérenguer C. Multi-branch hidden Markov models for remaining useful life estimation of systems under multiple deterioration modes. *Proceedings of the Institution of Mechanical Engineers, Part O: Journal of Risk and Reliability*. 2016; 230: 473-84.
30. Saxena A, Celaya J, Saha B, Saha S, Goebel K. On applying the prognostic performance metrics. *Annual conference of the prognostics and health management society*. 2009.

31. Kale AA, Haftka RT. Tradeoff of Weight and Inspection Cost in Reliability-Based Structural Optimization. *Journal of Aircraft*. 2008; 45: 77-85.
32. Kundu AK. *Aircraft design*: Cambridge University Press, 2010.
33. Kim NH, An D, Choi J-H. Prognostics and Health Management of Engineering Systems, An Introduction. Springer International Publishing, 2017, p. 347.
34. Cortie MB, Garrett GG. On the correlation between the C and m in the paris equation for fatigue crack propagation. *Engineering Fracture Mechanics*. 1988; 30: 49-58.
35. Bilir ÖG. The relationship between the parameters C and n of Paris' law for fatigue crack growth in a SAE 1010 steel. *Engineering Fracture Mechanics*. 1990; 36: 361-4.
36. RICE JA. Mathematical Statistics and Data Analysis. *Nelson Education*. 2006.
37. Huang B, Du X. Probabilistic uncertainty analysis by mean-value first order Saddlepoint Approximation. *Reliability Engineering & System Safety*. 2008; 93: 325-36.
38. Grewal MS, Andrews AP. Kalman Filtering: Theory and practice with Matlab, 4th Edition. *Wieley-Interscience, Canada*. 2014.
39. Wang Y, Binaud N, Gogu C, Bes C, Fu J. Determination of Paris' law constants and crack length evolution via Extended and Unscented Kalman filter: An application to aircraft fuselage panels. *Mechanical Systems and Signal Processing*. 2016; 80: 262-81.
40. Wang Y, Gogu C, Binaud N, Bes C. Predicting Remaining Useful Life by fusing SHM data based on Extended Kalman Filter. *Safety and Reliability of Complex Engineered Systems*: CRC Press, 2015, p. 2489-96.